

AD-A218 801

EXACT COPY

2

NAVAL POSTGRADUATE SCHOOL

Monterey, California



THESIS

A COMPARISON OF CuAlNi AND OTHER HIGH
DAMPING ALLOYS FOR THE PURPOSE OF
NAVAL SHIP SILENCING APPLICATIONS

by

Kenneth P. Roey

September 1989

Thesis Advisor:

Jeffrey A. Perkins

Approved for public release; distribution is unlimited

DTIC
ELECTE
MAR 8 1990
S B D

UNCLASSIFIED

SECURITY CLASSIFICATION OF THIS PAGE

Form Approved
OMB No 0704-0188

REPORT DOCUMENTATION PAGE

1a REPORT SECURITY CLASSIFICATION UNCLASSIFIED		1b RESTRICTIVE MARKINGS	
2a SECURITY CLASSIFICATION AUTHORITY		3 DISTRIBUTION AVAILABILITY OF REPORT Approved for public release; distribution is unlimited	
2b DECLASSIFICATION/DOWNGRADING SCHEDULE			
4 PERFORMING ORGANIZATION REPORT NUMBER(S)		5 MONITORING ORGANIZATION REPORT NUMBER(S)	
6a NAME OF PERFORMING ORGANIZATION Naval Postgraduate School	6b OFFICE SYMBOL (If applicable) Code 69	7a NAME OF MONITORING ORGANIZATION Naval Postgraduate School	
6c ADDRESS (City, State, and ZIP Code) Monterey, California 93943-5000		7b ADDRESS (City, State, and ZIP Code) Monterey, California 93943-5000	
8a NAME OF FUNDING SPONSORING ORGANIZATION	8b OFFICE SYMBOL (If applicable)	9 PROCUREMENT INSTRUMENT IDENTIFICATION NUMBER	
8c ADDRESS (City, State, and ZIP Code)		10 SOURCE OF FUNDING NUMBERS	
		PROGRAM ELEMENT NO	PROJECT NO
		TASK NO	WORK UNIT ACCESSION NO
11 TITLE (Include Security Classification) A COMPARISON OF CuAlNi AND OTHER HIGH DAMPING ALLOYS FOR THE PURPOSE OF NAVAL SHIP SILENCING APPLICATIONS			
12 PERSONAL AUTHOR(S) Roey, Kenneth P.			
13a TYPE OF REPORT Master's Thesis	13b TIME COVERED FROM TO	14 DATE OF REPORT (Year, Month, Day) 1989, September	15 PAGE COUNT 81
16 SUPPLEMENTARY NOTES The views expressed in this thesis are those of the author and do not reflect the official policy or position of the Department of Defense or the U.S. Government.			
17 COSATI CODES		18 SUBJECT TERMS (Continue on reverse if necessary and identify by block number)	
FIELD	GROUP	SUB-GROUP	
		Damping; Ship Silencing; Cu-Al-Ni	
19 ABSTRACT (Continue on reverse if necessary and identify by block number) Five high damping alloys, including TiNi, CuAlNi, CuZnAl, CuMn and FeCrMo, were heat treated to produce optimum damping conditions. The strain dependence of specific damping capacity was established using the resonant dwell technique. The results were compared with those of past investigations. For the CuAlNi alloy, six different heat treatment conditions were considered. The CuAlNi specimens were cold worked to determine the effect on damping. An industrial survey was conducted to determine the practicality of shipboard application of these alloys. A comparison of the advantages/disadvantages of each alloy was accomplished and recommendations were made for further study.			
20 DISTRIBUTION AVAILABILITY OF ABSTRACT <input checked="" type="checkbox"/> UNCLASSIFIED/AVAIL <input type="checkbox"/> SAME AS REP <input type="checkbox"/> DTIC USERS		21 ABSTRACT SECURITY CLASSIFICATION Unclassified	
22a NAME OF RESPONSIBLE INDIVIDUAL Prof. Jeffrey A. Perkins		22b TELEPHONE (Include Area Code) (408) 646-2216	22c OFFICE SYMBOL Code 69Ps

DD Form 1472, JUN 86

Previous editions are obsolete

S/N 0102-LE-014-6603

UNCLASSIFIED

Approved for public release; distribution is unlimited

A Comparison of CuAlNi and Other High Damping Alloys
for the Purpose of Naval Ship Silencing Applications

by

Kenneth Phillip Roey
Lieutenant Commander, United States Navy
B.S., United States Naval Academy, 1978

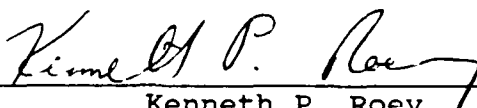
Submitted in partial fulfillment of the
requirements for the degree of

MASTER OF SCIENCE IN MECHANICAL ENGINEERING

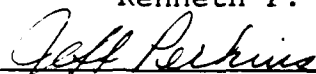
from the

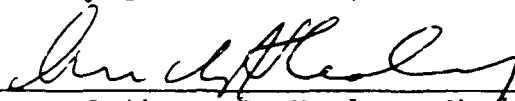
NAVAL POSTGRADUATE SCHOOL
September 1989

Author:


Kenneth P. Roey

Approved by:


Jeffrey A. Perkins, Thesis Advisor


Anthony J. Healey, Chairman
Department of Mechanical Engineering

ABSTRACT

Five high damping alloys, including TiNi, CuAlNi, CuZnAl, CuMn and FeCrMo, were heat treated to produce optimum damping conditions. The strain dependence of specific damping capacity was established using the resonant dwell technique. The results were compared with those of past investigations. For the CuAlNi alloy, six different heat treatment conditions were considered. The CuAlNi specimens were cold worked to determine the effect on damping. An industrial survey was conducted to determine the practicality of shipboard application of these alloys. A comparison of the advantages/disadvantages of each alloy was accomplished and recommendations were made for further study.

iii

Accession For	
NTIS GRA&I	<input checked="checked" type="checkbox"/>
DTIC TAB	<input type="checkbox"/>
Unannounced	<input type="checkbox"/>
Justification	
By	
Distribution/	
Availability Codes	
Dist	Avail and/or Special

A-1

TABLE OF CONTENTS

I.	INTRODUCTION -----	1
	A. GENERAL -----	1
	B. OBJECTIVES -----	1
	C. BACKGROUND -----	2
II.	EXPERIMENTAL PROCEDURE -----	5
	A. EQUIPMENT -----	5
	B. MATERIAL -----	9
III.	RESULTS AND DISCUSSION -----	16
	A. DAMPING COMPARISONS -----	16
	B. EQUIPMENT -----	31
IV.	ENGINEERING APPLICATIONS -----	35
	A. GENERAL -----	35
	B. SPECIFIC ALLOY SYSTEMS -----	35
V.	CONCLUSIONS AND RECOMMENDATIONS -----	44
	A. CONCLUSIONS -----	44
	B. RECOMMENDATIONS -----	45
APPENDIX A:	PROCEDURE FOR READING STRAIN MEASUREMENTS -----	46
APPENDIX B:	TABLES OF MATERIAL PROPERTIES -----	48
APPENDIX C:	LIST OF ADDRESSEES -----	68
	LIST OF REFERENCES -----	71
	INITIAL DISTRIBUTION LIST -----	74

LIST OF TABLES

2.1	SDC SPECIMEN DIMENSIONS -----	11
2.2	HEAT TREATMENT CONDITIONS -----	11
2.3	BULK ANALYSIS OF CuAlNi ALLOY (WT%) -----	13
3.1	PEAK DAMPING VS. STRAIN -----	29

LIST OF FIGURES

1.1	Half Power Point Method -----	4
2.1	Block Diagram of Test Apparatus -----	6
2.2	Resonant Dwell Apparatus -----	7
2.3	Specifications for Damping Specimens -----	10
2.4	Phase Diagram for a Cu-Al-3Ni Alloy -----	14
3.1	SDC vs. Strain for FeCrMo -----	17
3.2	SDC vs. Strain for TiNi -----	18
3.3	SDC vs. Strain for CuMn -----	20
3.4	SDC vs. Strain for CuZnAl -----	21
3.5	SDC vs. Strain for CuAlNi, No Aging -----	23
3.6	SDC vs. Strain for CuAlNi, Aged @ 150 C/1 Hour --	24
3.7	SDC vs. Strain for CuAlNi, Aged @ 200 C/1 Hour --	25
3.8	SDC vs. Strain for CuAlNi, No Aging (BW Quench) -	26
3.9	SDC vs. Strain for CuAlNi, Aged @ 150 C/1 Hour (BW Quench) -----	27
3.10	SDC vs. Strain for CuAlNi, Aged @ 200 C/1 Hour (BW Quench) -----	28

I. INTRODUCTION

A. GENERAL

Research into the use of high damping materials for ship silencing applications has been conducted at the Naval Postgraduate School (NPS) over the last 15 years. The common goal of this research has been to identify promising materials which might reduce the level of noise entering the water. In an age when the past leader and architect of the Soviet Navy has predicted the advent of very deep diving submarines with speeds in excess of 100 knots by the turn of the century, it becomes imperative that the U.S. Navy maintains its acoustical advantage over all potential adversaries.

B. OBJECTIVES

The purpose of this current research was to develop a data base of damping characteristics of the CuAlNi alloy system, to compare it to other previously tested high damping alloys, and to evaluate the practicality of their use in a shipboard environment. A secondary objective of the research was to find ways to improve the damping test apparatus in order to fully utilize the capabilities of the electromagnetic shaker and obtain more complete damping profiles of the respective alloys.

C. BACKGROUND

The search for effective high damping materials with good mechanical properties has been pursued by industry and government agencies alike. The motivation for these efforts includes the advent of new tougher OSHA standards, improved service life of machinery components due to reduction of fatigue, military related noise reduction considerations, and even the possibility of use in earthquake protection. Marine applications of high damping alloys have been rather limited, though the Cu-Mn alloy SONOSTON, developed by Stone Manganese Marine Ltd. of England, has been supplied to nine NATO navies since the 1970's for ships propellers.

The currently available high damping materials fall into three major categories, whose features may be summarized as follows:

1. Ferromagnetic--Amplitude dependent, frequency independent damping due to magnetostrictive movement of Bloch walls [Ref. 1]. Examples include alloys from the FeCrMo and FeCrAl alloy systems.
2. Shape Memory--Amplitude dependent, frequency independent damping due to movement of internal martensitic twin boundaries. Examples include CuMn and CuAlNi.
3. Stress Relaxation--Amplitude independent, frequency dependent damping due to the stress induced motion of planar boundaries [Ref. 2]. Examples include ZnAl and FeCSi.

Damping measurements of these high damping materials have commonly been accomplished by use of either the torsional pendulum or by the cantilever beam resonant dwell technique. Over the last several years, Perkins, et al.

have refined the use of the resonant dwell method at the Naval Postgraduate School. The half power point method has been used to quantify the damping factor (Figure 1.1). Using this method the quality factor (Q) is defined as:

$$Q = \omega_n / (\omega_2 - \omega_1)$$

The specific damping capacity (SDC) of a material may then be defined as:

$$SDC(\%) = 200\pi Q^{-1}$$

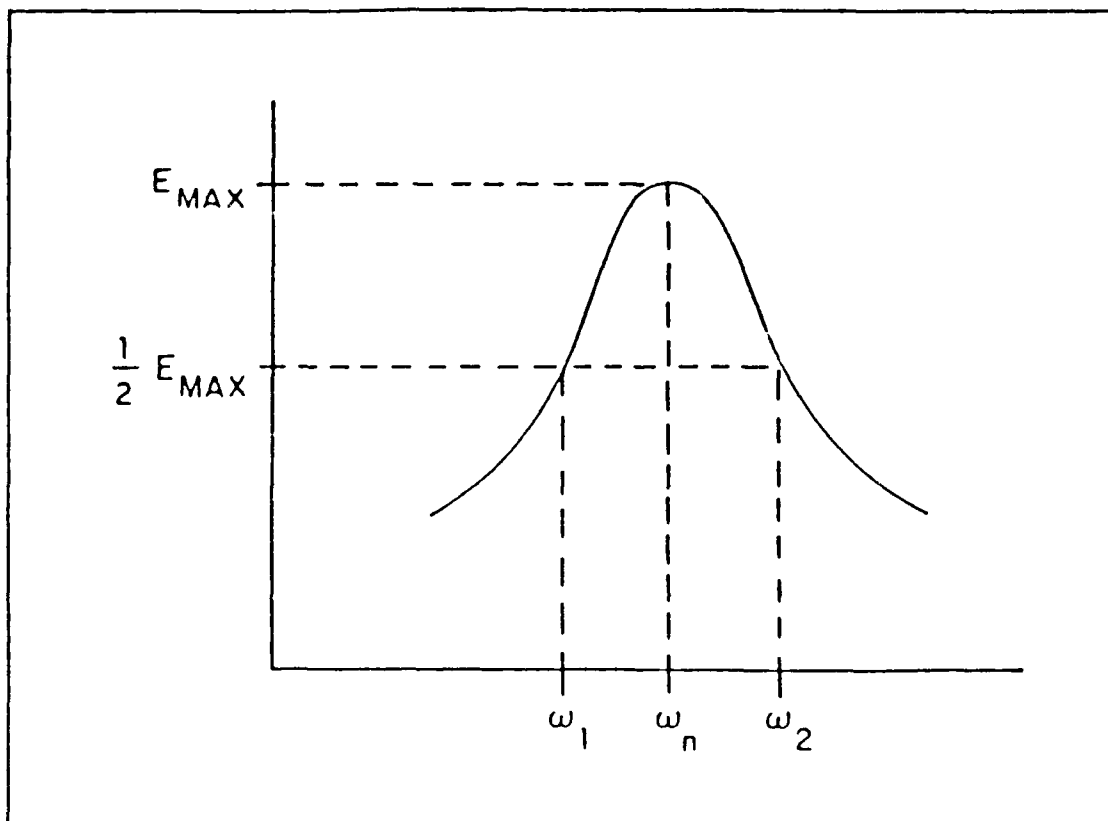


Figure 1.1 Half Power Point Method

II. EXPERIMENTAL PROCEDURE

A. EQUIPMENT

The testing apparatus used for the damping capacity measurements was based on a modified design of the method developed by J.C. Heine of Bolt, Beranek and Newman [Ref. 3]. The layout of this design is shown diagrammatically in Figure 2.1 and a schematic of the base and cantilever beam structure is depicted in Figure 2.2. The system consists of the SD-380 Spectral Dynamics Signal Analyzer sending a pseudo-random noise signal to the SS-250 Power Amplifier, which in turn controls the input to the Modal 50A Electromagnetic Exciter. The response of the structure is measured by the input accelerometer and this signal is amplified by a Model 4416A Signal Conditioner prior to return to the Signal Analyzer via channel A. The response of the cantilever beam is measured by a strain gage mounted at the root of the beam, output of which is connected to the BAM-1 Bridge Amplifier and Meter and then through a TRMS Multimeter to channel C of the Signal Analyzer.

The decision to use a strain gage for both output response and strain amplitude measurements was based on prior work done at NPS. Heil [Ref. 4] had shown that use of either the strain gage or a beam tip accelerometer produced nearly identical results. The work of Cronauer [Ref. 5] and

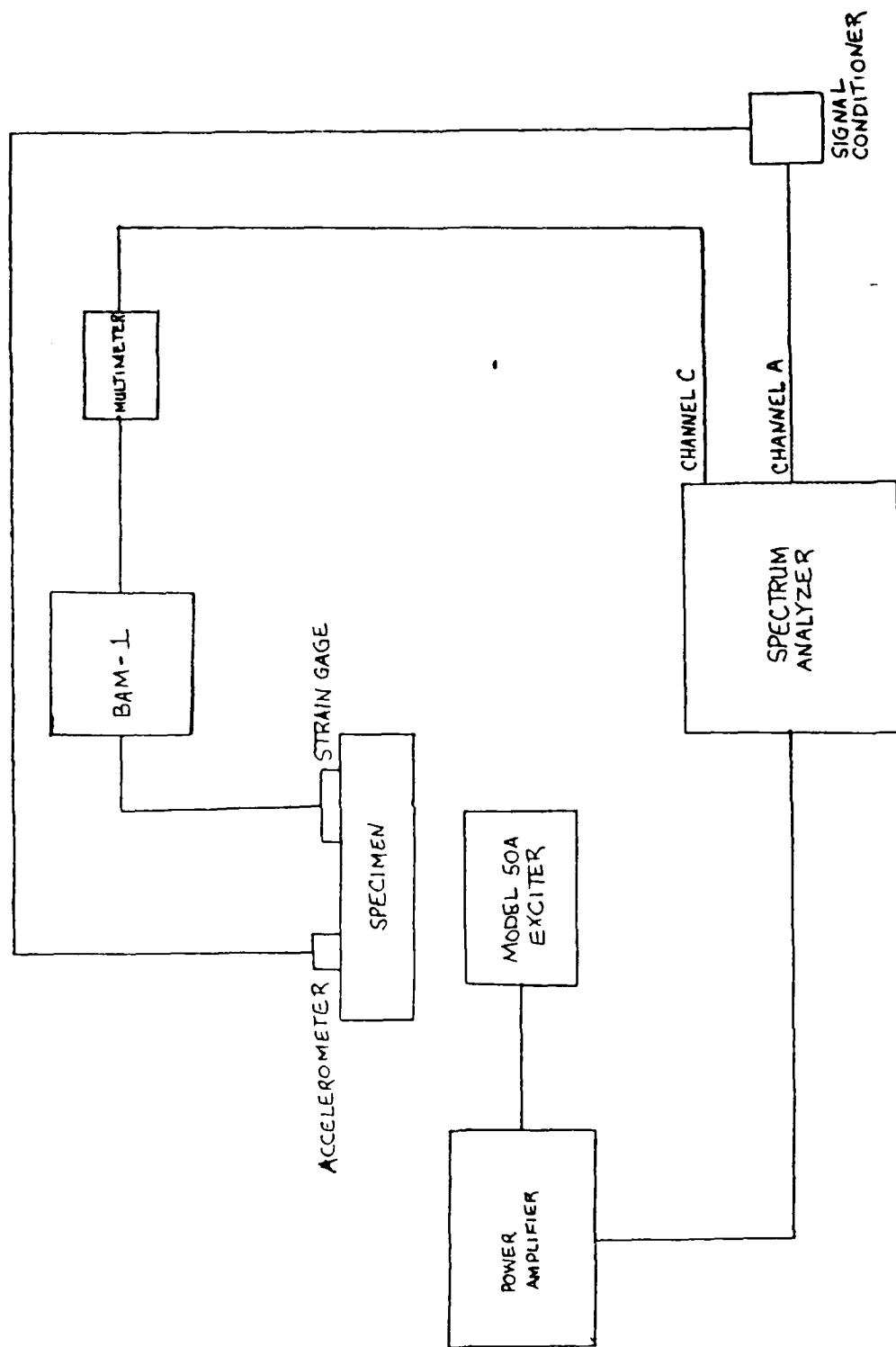


Figure 2.1 Block Diagram of Test Apparatus

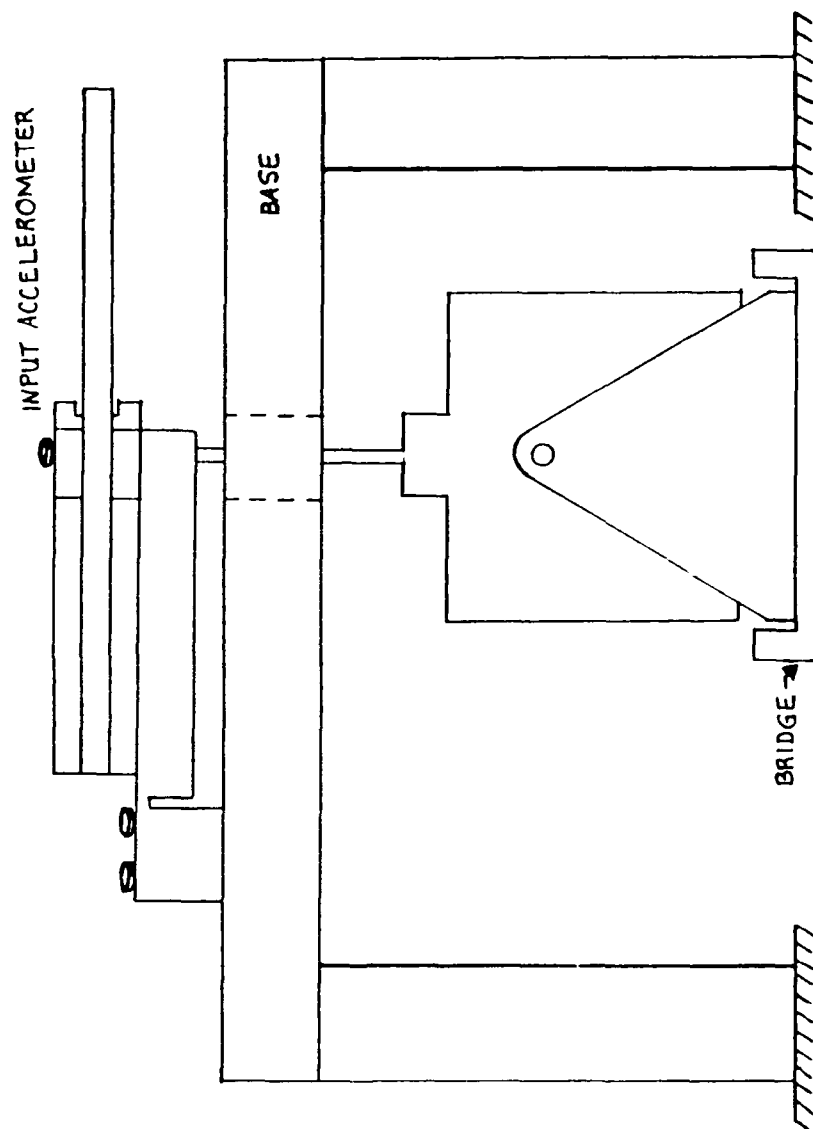


Figure 2.2 Resonant Dwell Apparatus

others indicated that the use of the first modal response was sufficient to characterize the beam damping. Other researchers have also used the fundamental mode of vibration due to practical limitations of the test apparatus [Ref. 6].

One of the objectives of this research was to integrate the more powerful Modal 50A Exciter into the existing test apparatus. Some minor modifications were made to the stinger assembly, but the shaker was otherwise completely compatible with the existing installation. The power amplifier has a range of 30 settings. Input levels to the damping apparatus are described here in a notation such as 0.5/15, where the first number indicates the output voltage from the Signal Analyzer and the second number the setting of the amplifier. Prior to conducting damping measurements, each beam was instrumented with a precision strain gage with a gage factor of $2.12 \pm 0.5\%$. Calibration of the gages prior to each run was conducted in accordance with Appendix A. Throughout the experiment, the average target count (N) was set at 200 and the Hanning weighting function was used to process the data.

In attempting to replicate previously obtained damping curves, it became evident that the primary high damping mechanisms were activated only when above certain threshold stress levels. The particular threshold stress level was dependent on the particular alloy and treatment condition. For example, for the FeCrMo system, input voltages of 0.1 V

(and corresponding small tip deflections of half an inch or less) were sufficient to activate high damping. On the other hand, for the CuMn and CuAlNi alloys, input voltages of 0.5 V (and tip deflections of two inches or more) were necessary. The maximum input setting used throughout the experiments was 0.5/25, which corresponded to approximately 2000 microstrain. At this level coherence became unacceptable, strain gages failed after only a few cycles and the spring steel piece used to pivot the beam assembly from the base structure became susceptible to failure. However, it was determined that the amplifier was capable of input levels approaching 1.0/25 prior to overloading. Therefore, in order to fully utilize the capabilities of the shaker, it will be necessary to further modify the current testing apparatus.

B. MATERIAL

All measurements were conducted at room temperature. The specimens used were all cut in the geometry shown in Figure 2.3. Table 2.1 gives the dimensions of the various beams and Table 2.2 summarizes the various heat treatments performed on each specimen. Heat treatments were chosen which would produce optimum damping, based on previous research. All of the beams, with the exception of the CuAlNi, had been previously used in other work and were retreated for the present experiments. All specimens were stored in a freezer following their respective heat

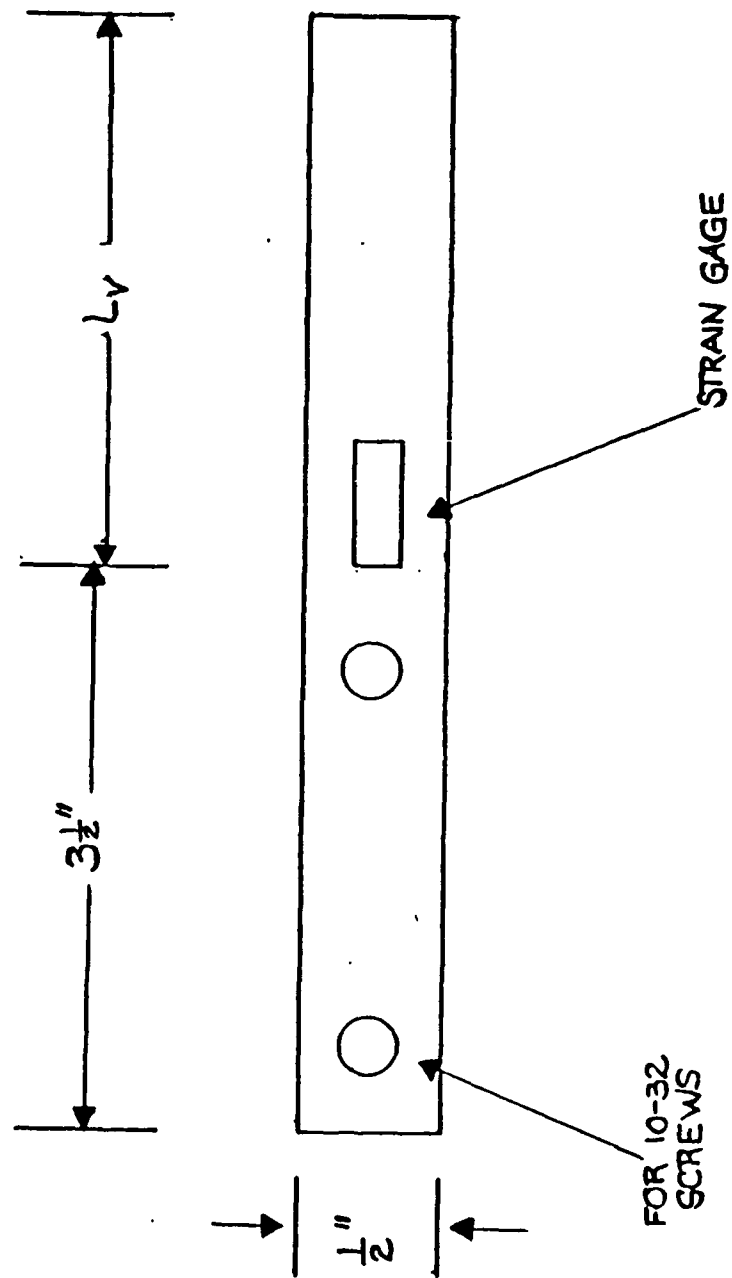


Figure 2.3 Specifications for Damping Specimens

TABLE 2.1

SDC SPECIMEN DIMENSIONS

ALLOY	THICKNESS (INCHES)	WIDTH (INCHES)	VIBRATING LENGTH (INCHES)
CuAlNi	.08	.51	5.24
CuMn	.06	.50	4.69
CuZnAl	.07	.50	4.47
FeCrMo	.06	.51	6.97
TiNi	.07	.53	5.06

TABLE 2.2

HEAT TREATMENT CONDITIONS

Alloy	Treatment
CuAlNi	<p>Solution treat at 800° C for 30 minutes, quench to room temperature. One sample to be tested in unaged condition, one sample aged at 150° C for 1 hour and a third sample aged at 200° C for 1 hour.</p> <p>Alternate Treatment: Solution treat at 800° C for 30 minutes, quench to boiling water, quench to room temperature. Aging conditions as above.</p>
CuZnAl	<p>Solution treat at 900° C for 20 minutes, quench to 150° C for 10 minutes, quench to room temperature.</p>
TiNi	As cast.
CuMn	<p>Solution treat at 800° C for 2 hours, quench to room temperature. Age at 400° C for 16 hours. Retain sample in freezer until ready for use.</p>
FeCrMo	<p>Solution treat at 1100° C for 1 hour, furnace cool to room temperature.</p>

treatments, this in order to prevent any room temperature aging effects, such as those which are well-known to occur in the CuMn alloy system.

Cronauer indicated that the proper heat treatment for the CuZnAl system included sequential step quenching to room temperature. Delaey [Ref. 7], states that step quenching at a temperature just below the critical ordering temperature has been shown to favor the growth of ordered DO₃ rosettes in a disordered matrix. This ordering is crucial to obtaining a high damping condition. Therefore, it was concluded that the treatment indicated in Table 2.2 was appropriate.

Several sheets of CuAlNi alloy in the untreated condition were provided by Memory Metals, Inc., Stamford, CT. Chemical analysis of the material was performed by Anamet Laboratories of Hayward, CA, and the results are presented in Table 2.3. Memory Metals, Inc. recommended solution treating the samples at 800° C for 30 minutes, quenching to room temperature and then aging at 150° C for 1 hour. Figure 2.4, a phase diagram for a near composition CuAlNi alloy indicates that this treatment should produce a martensitic structure capable of high damping. In order to observe the effects of aging on the damping and microstructure, it was decided to age specimens at both 150° C and 200° C. Also specimens quenched to room temperature with no aging were examined.

TABLE 2.3

BULK ANALYSIS OF CuAlNi ALLOY (WT%)

Copper	80.1
Aluminum	11.87
Nickel	4.95
Manganese	1.83
Titanium	1.05
Remainder	0.2

Machining of the CuAlNi specimens proved quite difficult due to their extreme hardness in the untreated condition. Once machining was completed, the specimens were sealed in evacuated glass tubes, in which they remained until water quenching. It was found that using this method the beams underwent pronounced warping, due to uneven cooling following the breakage of the glass as it entered the water quench bath. To prevent this problem from occurring, the beams were treated without enclosure. No surface oxide problem was encountered and warping was minimal, as long as a near zero degree contact angle was maintained when entering the water quenchant.

Even without being sealed in the tubes, it was evident that relatively large residual stresses existed in the CuAlNi beams. This effect is noted by Miyazaki [Ref. 8]. It was suggested that when the martensite start (M_s) temperature was close to that of the quenching media, the

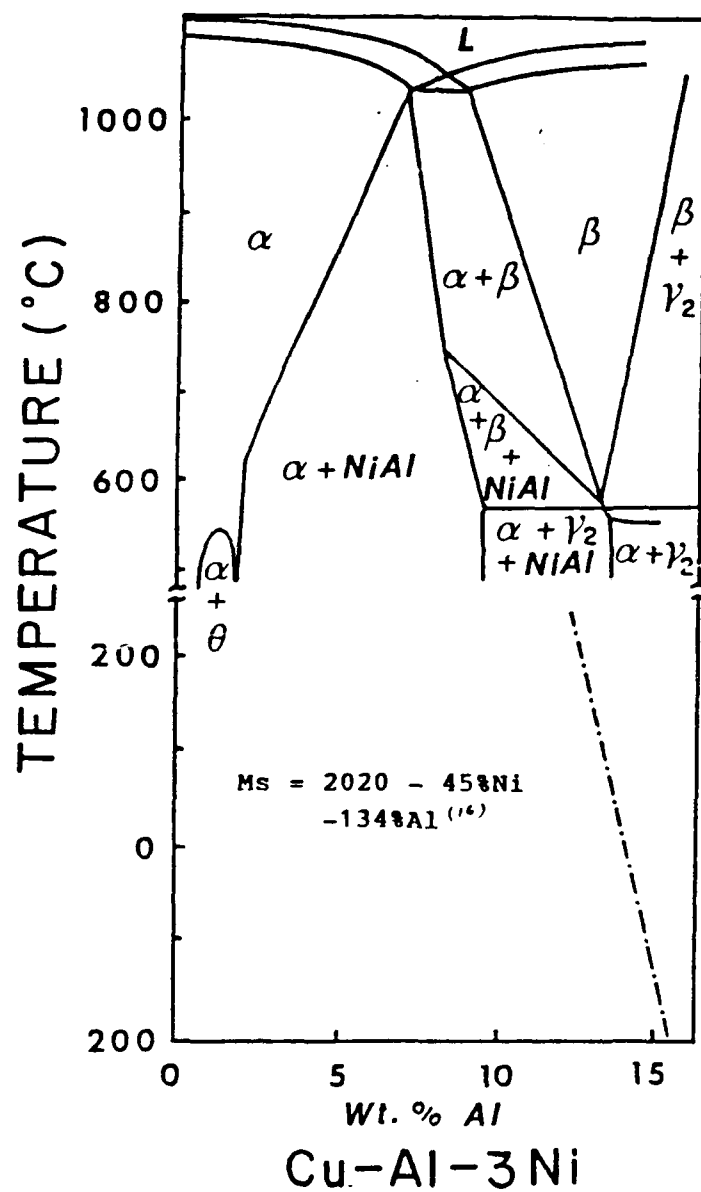


Figure 2.4 Phase Diagram for a Cu-Al-3Ni Alloy

resultant lower thermal stresses eliminated cracking. The CuAlNi alloy being used was known to have a M_s temperature near 125° C. Therefore, it was decided to use a boiling water quench prior to quenching to room temperature. This method worked well and produced beams without any visible signs of warpage.

Another aspect of this research involved cold rolling the CuAlNi beams in order to determine the effect this might have on damping. Initially, several of the beams were given a 10% cold roll and then retested. It was determined that the previously demonstrated high damping properties of CuAlNi had been virtually completely eliminated and it was decided to attempt to determine the threshold at which high damping was no longer apparent. Therefore, a beam which had been quenched to room temperature without aging was reduced in thickness in 1% increments and retested at each interval until no appreciable damping was evident.

III. RESULTS AND DISCUSSION

A. DAMPING COMPARISONS

1. FeCrMo

Figure 3.1 demonstrates an increase of specific damping capacity (SDC) with increasing cyclic strain amplitude to a maximum of about 65% SDC at approximately 100 microstrain, followed by a drop in damping; the data is presented over the full range of accuracy of the equipment. O'Toole [Ref. 9], found this same relationship, with a peak SDC of 55% at about 75 microstrain. Cronauer determined that the peak SDC of 65% occurred at about 5 microstrain. Though unable to drive the stresses past the peak with the lower powered shaker, Cronauer postulated that a saturation of the damping would occur due to restricted movement of magnetic domain walls and dislocations. This hypothesis seems to be a plausible explanation for the observed data. It would be interesting to find whether this decrease in damping continued to some minimum and leveled off or if the damping properties were continually diminished as strain increased past the point of peak damping.

2. TiNi

Figure 3.2 demonstrates an increase of SDC with increasing cyclic strain amplitude to a maximum of 55% SDC at about 500 microstrain. The damping of the material

FE(84.7)CR(11.3)MO(2.5)-(W%)

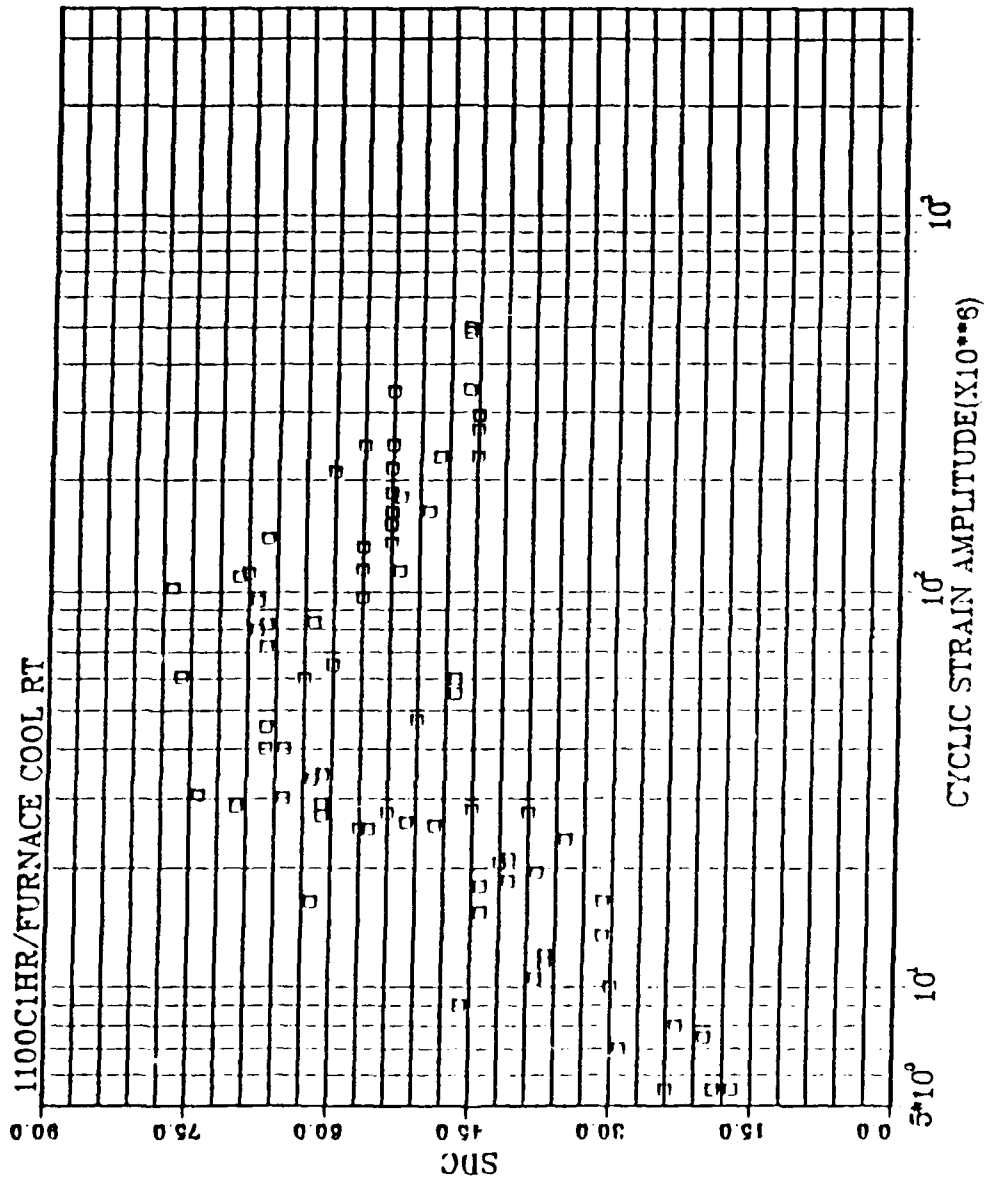


Figure 3.1 SDC vs. Strain for FeCrMo

Ti(44.5)Ni(43.4)Cu(12.1)-(W%)

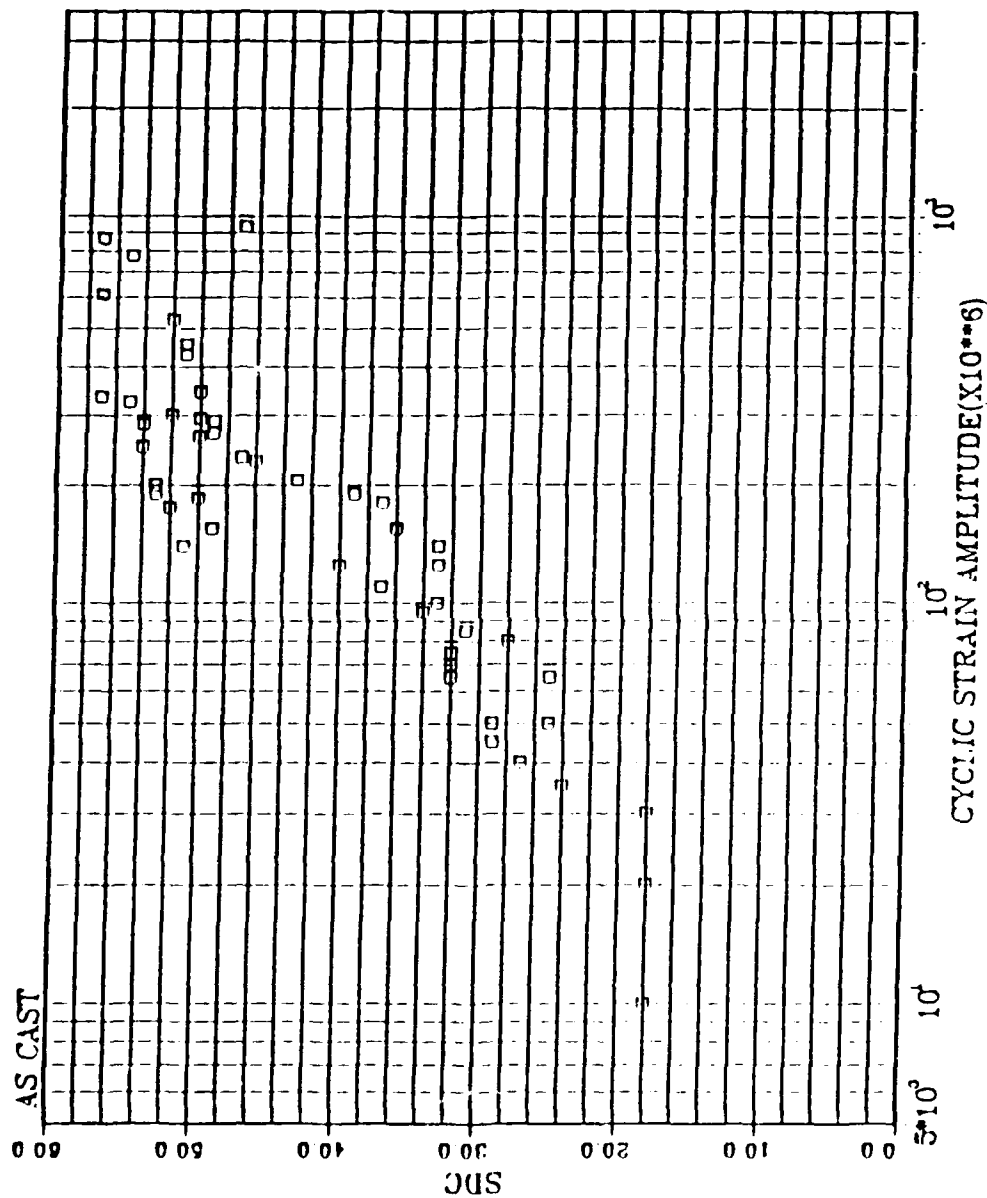


Figure 3.2 SDC vs. Strain for TiNi

seemed to level off at this point, though it is unclear whether the SDC might actually decrease beyond the peak. Cronauer obtained similar results, finding a peak SDC of 47.6% at 15.3 microstrain. The coherence of the data points obtained was excellent and there was little scatter. The high damping properties of this material in the as cast condition is due to lattice friction stemming from motion of the martensite twin boundaries.

3. CuMn

Figure 3.3 shows a clear linear type relationship between damping and strain amplitude upon activation of the high damping mechanism. A maximum of 52% SDC was achieved at a value of 1800 microstrain. These values are in very close agreement with those of Reskusion [Ref. 10], as well as those of Heil. Cronauer was again unable to reach these high values of strain, but extrapolation of that data suggests that the same results would have been obtained. A peak in the damping would be expected at some point, but equipment limitations again frustrated attempts at defining it.

4. CuZnAl

Figure 3.4 indicates the presence of high damping in this heat treatment condition. A maximum of 32% SDC at about 150 microstrain was observed. There was some problem with data scatter and poor coherence of individual points, and runs were repeated as necessary to achieve a higher

CU(53.1)MN(44.8)AL(1.6)-(W%)

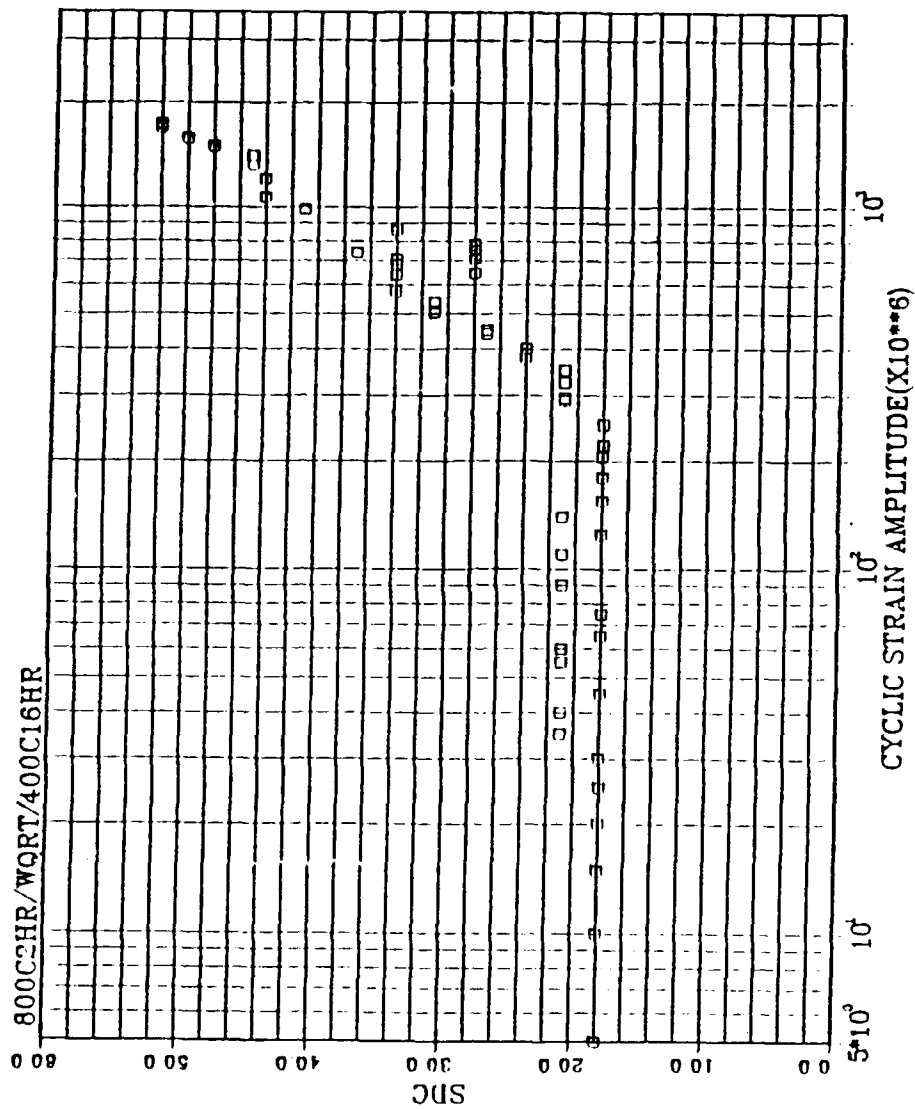


Figure 3.3 SDC vs. Strain for CuMn

900C20MIN/Q150C10MIN/WQRT

SDC

CYCLIC STRAIN AMPLITUDE(X10**6)

10⁻⁶ 10⁻⁵ 10⁻⁴

Figure 3.4 SDC vs. Strain for CuZnAl

confidence in the data. Previously, Cronauer reported no significant damping achieved in this alloy. However, the heat treatment utilized in Cronauer's work included solution treating at 900° C for 20 minutes followed by a direct water quench to room temperature. For such a treatment of this alloy, the degree of long-range order appears to be the major factor affecting M_s [Ref. 11]. If the equilibrium degree order is not achieved the M_s may be reduced, and what would normally appear to be a satisfactory heat treatment to produce a martensitic high damping structure will produce something quite different. Ahlers [Ref. 12] states that step quenching reduces the quenched in disorder and eliminates excess vacancies. By controlling the equilibrium order of the structure, improved damping is possible, as well as stabilization of the mechanical properties of the material.

5. CuAlNi

Figures 3.5-3.10 are the strain versus damping graphs for the six different heat treatment conditions. All test specimens demonstrated a baseline damping of about 15% prior to activation of high damping. Once activated, SDC increased with strain, in most cases in a fairly linear fashion. Peak damping for each condition is summarized below in Table 3.1.

From this data, two generalizations can be made. First, those samples which were quenched to boiling water

CU(80)AL(12)NI(5)MN(2)TI(1)-(W%)

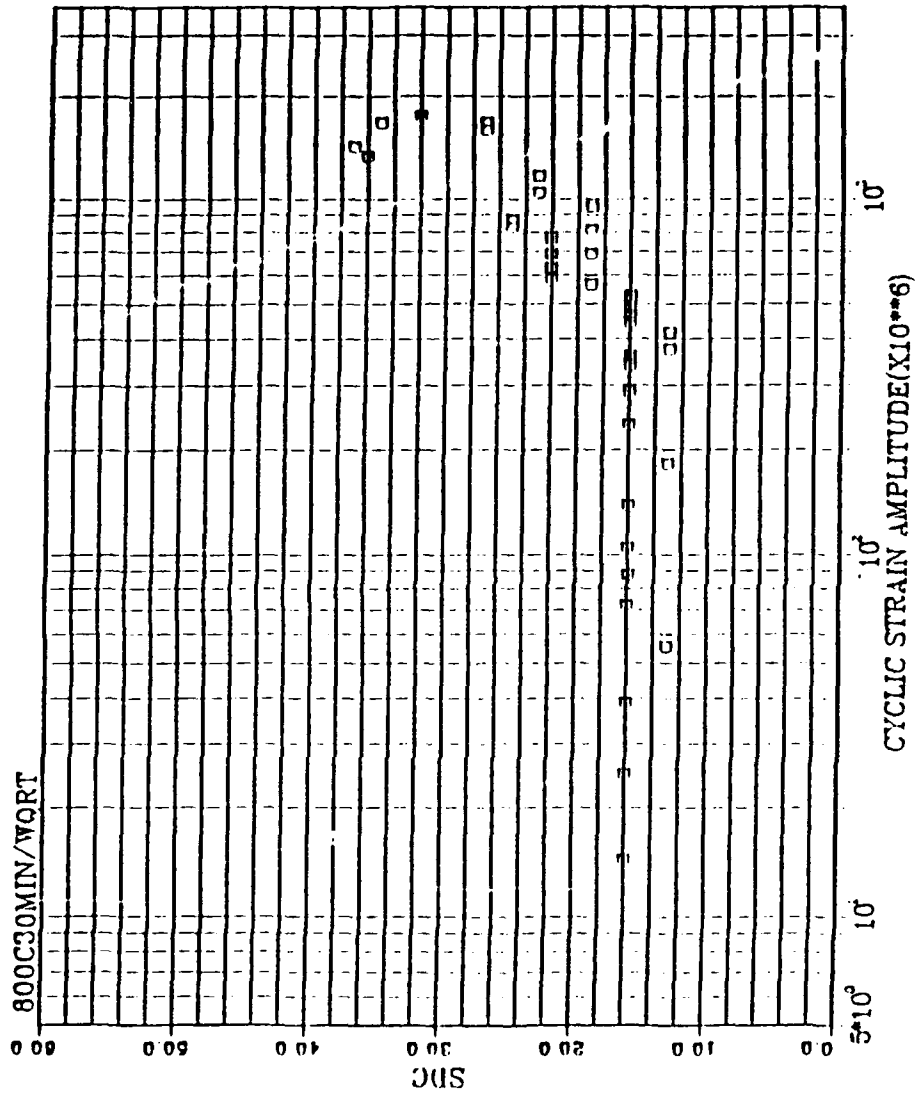


Figure 3.5 SDC vs. Strain for CuAlNi. No Aging

CU(80)AL(12)NI(5)MN(2)TI(1)--(W%)

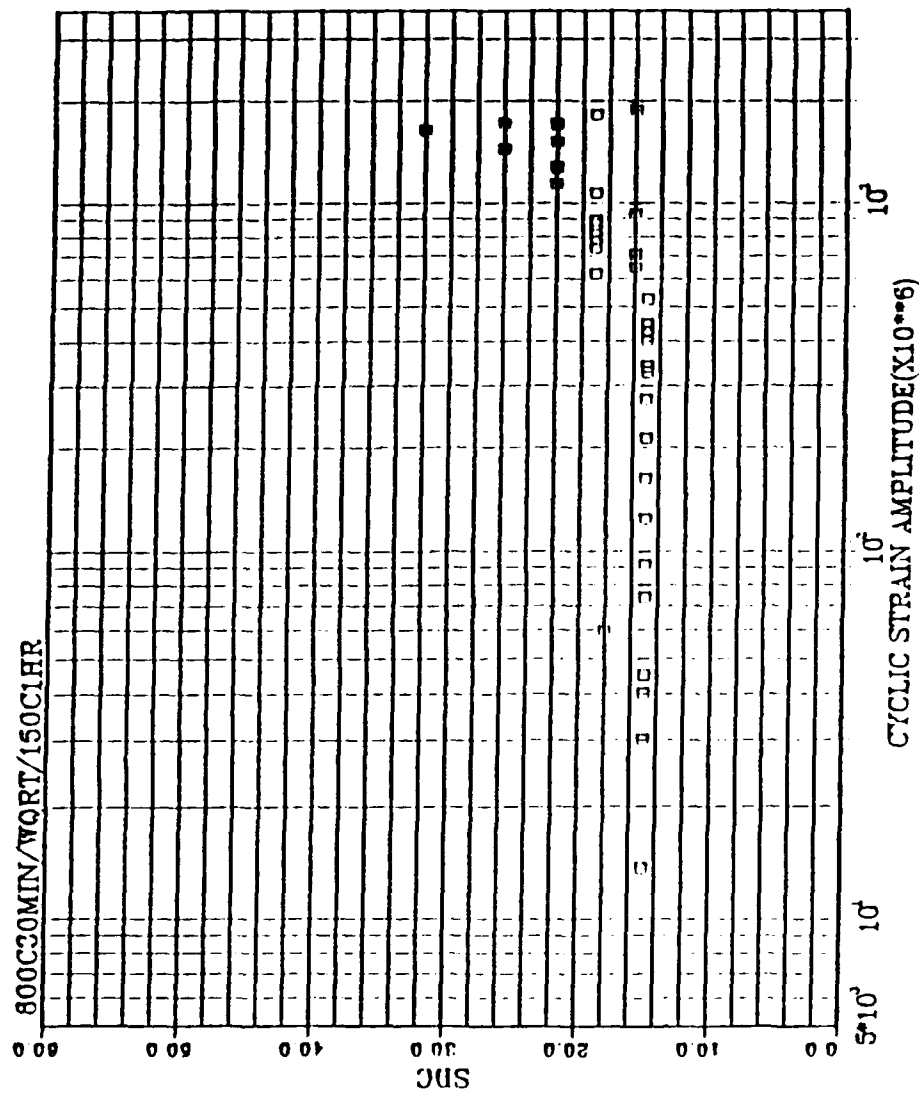


Figure 3.5 SDC vs. Strain for CuAlNi, Aged @ 150 C/1 Hour

Cu(80)AL(12)NI(5)MN(2)TI(1)-(W%)

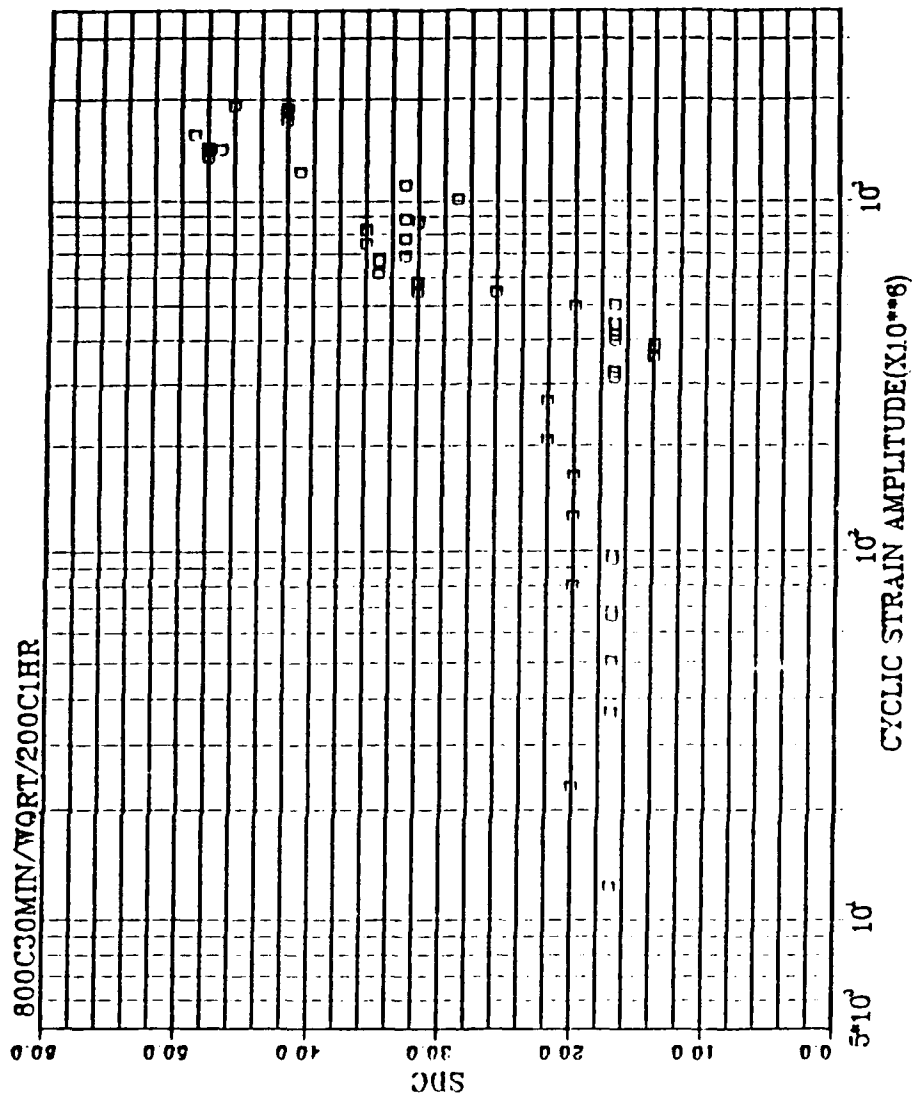


Figure 3.7 SDC vs. Strain for CuAlNi, Aged @ 200 C/1 Hour

CU(80)AL(12)NI(5)MN(2)TI(1)-(W%)

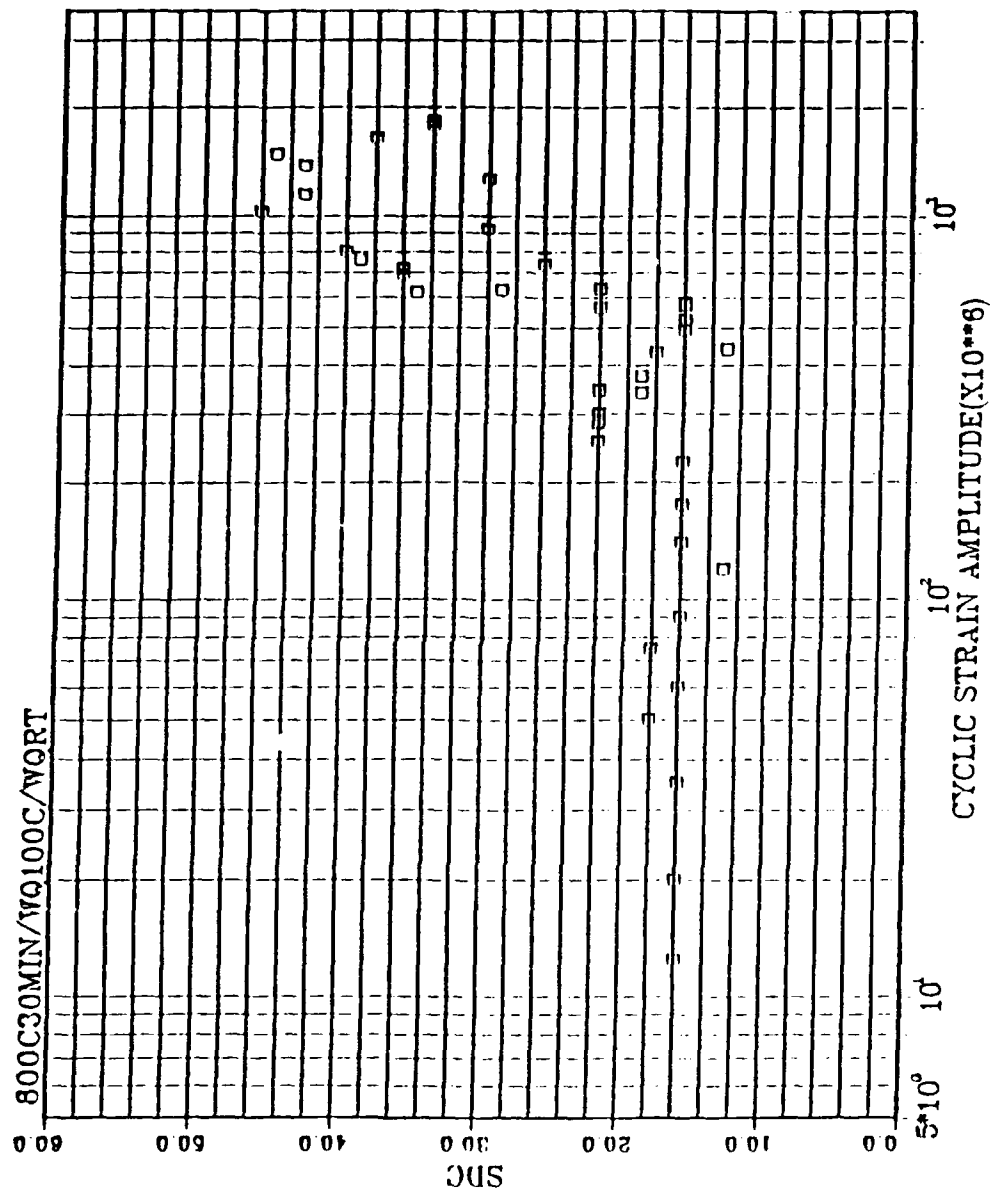


Figure 3.8 SDC vs. Strain for CuAlNi, No Aging (BW Quench)

CU(80)AL(12)NI(5)MN(2)TI(1)-(W%)

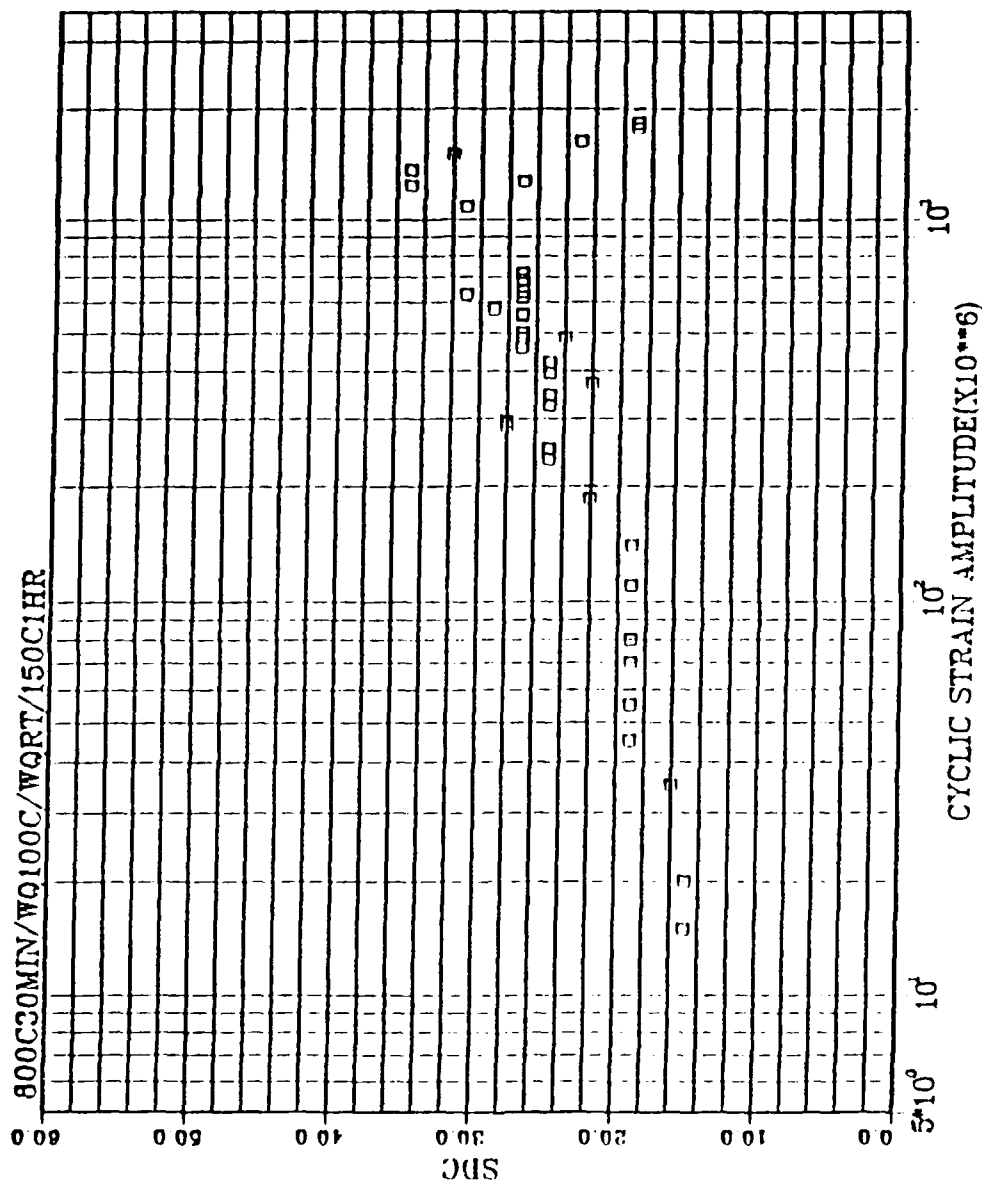


Figure 3.9 SDC vs. Strain for CuAlNi. Aged @ 150 C/1 Hour (BW Quench)

CU(80)AL(12)NI(5)MN(2)TI(1)-(W%)

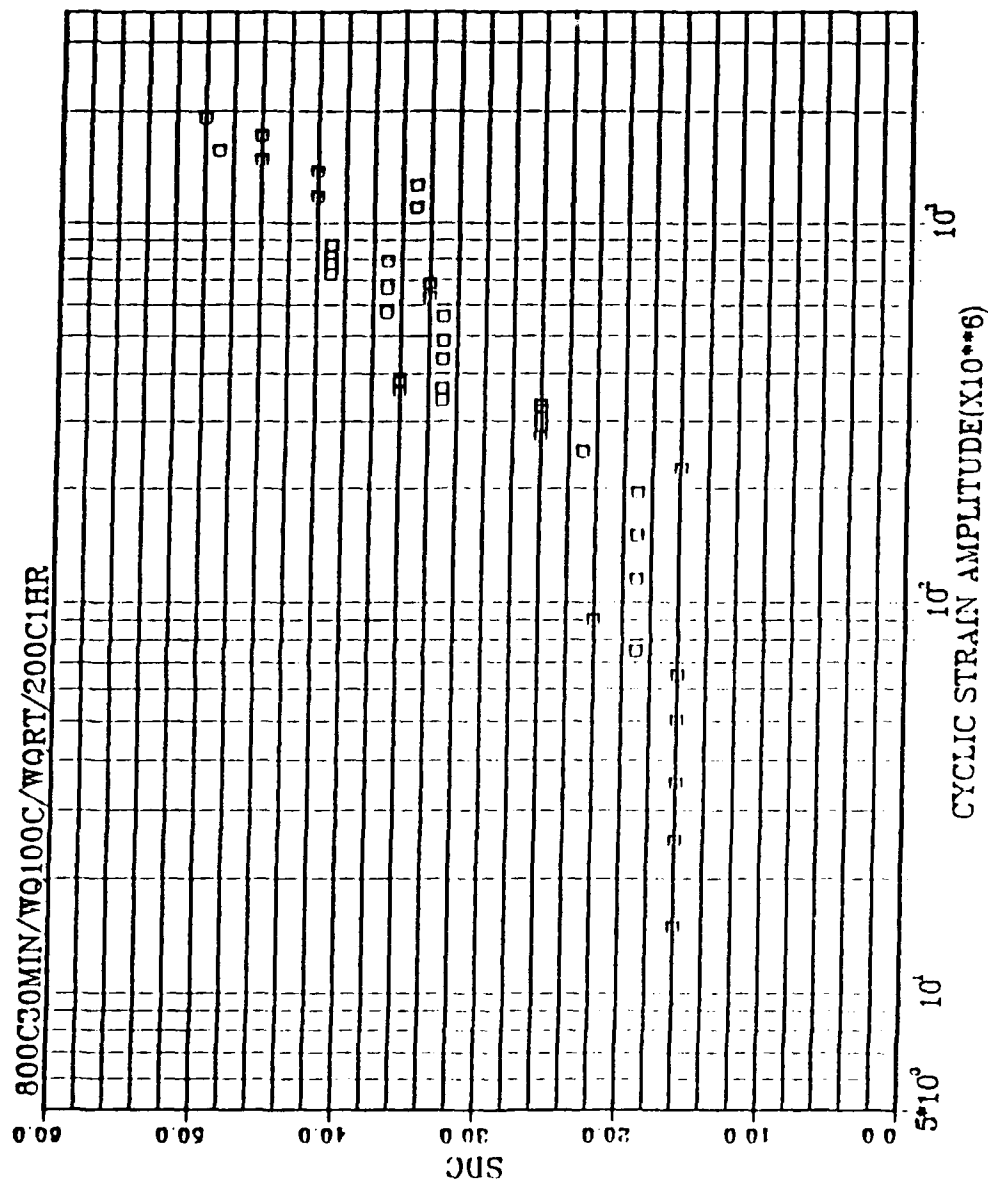


Figure 3.10 SDC vs. Strain for CuAlNi. Aged @ 200 C/1 Hour (BW Quench)

TABLE 3.1

PEAK DAMPING VS. STRAIN

Aging Condition	Peak SDC (%)	Strain @ Peak
No aging	36	1500
150 ⁰ C/1 hour	28	1550
200 ⁰ C/1 hour	49	1000
No aging (BW quench)	45	1200
150 ⁰ C/1 hour (BW quench)	34	1300
200 ⁰ C/1 hour (BW quench)	50	2000

prior to quenching to room temperature showed slightly elevated damping over those quenched directly to room temperature. Secondly, the samples aged at 150⁰ C demonstrated significantly lower damping than the other two treatment conditions. Input power levels to achieve a certain level of strain were similar in all cases.

Transmission electron microscopy (TEM) examinations recently carried out by Rappeline [Ref. 13], revealed no significant observable variations in microstructure between the different treatment conditions. It is possible that differences in vacancy concentrations, or subtle differences in ordering, which are not observable using standard TEM imagery techniques, are responsible for the variation in damping. Rappeline also studied the variations of M_s with aging condition, using differential scanning calorimetry.

The calorimetry results indicated that a much larger energy of transformation was exhibited by the samples aged at 200° C, which may be related to the differences in damping. See Rappeline [Ref. 13] for a detailed explanation of the microstructural effects on damping.

The final aspect of the present experiments consisted of cold working some of the previously tested CuAlNi beams. Initially, beams which had been aged at 150° C and 200° C were given a 10% cold roll, then reinstrumented and tested. High damping was virtually entirely eliminated, though the baseline 15% damping remained. Next, beams with no aging treatment were given incremental 1% cold rolls and were retested for damping at each interval. It was evident that the damping was reduced at greater values of cold work, but the quality of measurements were poor and it was impossible to pick out the exact point where high damping was completely eliminated. In any case, it is clear that a significant reduction in damping occurs at small amounts of cold work. This effect has also been shown for alloys such as FeCrMo, which rely on magnetomechanical damping, where cold work values of less than 1% dramatically reduce the damping effect [Ref. 14].

It was noted that following cold rolling of the beams cracks appeared, which in some cases allowed portions of the beams to be broken off easily by hand via an intergranular fracture mechanism. This problem will be

addressed later in the Engineering Analysis section. In addition, as cold rolling progressed, greater input levels were required to reach the same values of strain, reflecting the changing modulus of the material. It thus became more difficult to determine whether high damping had actually been eliminated or if it had been merely pushed "to the right," i.e., that it would have been activated at higher strain levels.

B. EQUIPMENT

As stated previously, at input power levels greater than 0.5/25 it was found that strain gages had a short life and coherence became a great problem. In order to extend the range of testing of the various materials, some changes must be made to the damping apparatus. One alternative is to resume use of the torsional pendulum, which had been used in damping research up until several years ago at NPS [Ref. 15]. The major disadvantage of this method is that it is only capable of measuring damping at low frequencies. However, if it was known beforehand that the materials damping mechanism was frequency independent, this would not be a great drawback. Nash and Schwaneke [Ref. 16] have developed a digital instrumentation package for the torsion pendulum which decreases the time required to obtain data, while at the same time increasing its accuracy. The system as designed allows it to be connected directly to a micro-computer for real time data analysis.

Returning to the present apparatus, the weak link of the system appears to be the strain gages. Not only do they fail with great regularity, but mounting them is a time consuming process and they require a protective coating which takes 24 hours to cure properly. An output accelerometer would easily provide damping data, but a means of measuring the stress or strain amplitude would still be required. Use of an optical measuring device to determine beam tip deflection can provide a measure of both damping and peak stress, as devised by Heine. Using this scheme, an input accelerometer is still required, along with some means of knowing the modulus of the material. Modulus information could be easily supplied by tensile testing.

Another option is use of a magnetic eddy current sensor to determine beam tip amplitude. A relatively simple apparatus could be designed allowing movement of the sensor dependent on the power input levels. This is necessary due to the approximately half inch effective range of these type sensors.

The apparatus used by Kaufman [Ref. 17] included a stroboscope which facilitated optical measurement with a low power microscope with a retical. It was used in conjunction with an environmental chamber with a range of operation between -100° C and $+300^{\circ}$ C. A high quality microscope of this type could be purchased for several hundred dollars and could easily be adapted to the present setup. The currently

used environmental chamber at NPS is capable only of heating from room temperature to approximately $+115^{\circ}$ C, and would have to be modified to allow visual observation of the samples. Calorimetry conducted by Rappeline indicated Ms temperatures in excess of 140° C for the CuAlNi alloy, which makes the current chamber of little value in monitoring changes in damping versus temperature, i.e., phase transformations. A commercially available environmental chamber similar to that used by Kaufman would cost approximately \$25,000.

A final alternative is the use of a Dynamic Mechanical Thermal Analyzer (DMTA), such as the one currently used by the David Taylor Research Center. Primarily used in the study of polymers, the DMTA can be used to measure damping as a function of strain over a wide range of frequency and temperature. Small bar samples are vibrated sinusoidally and both stress and strain are measured. The phase lag of strain behind stress is translated into a mechanical loss factor, by decomposing the complex modulus into storage and loss moduli. Coupled with a data acquisition system and appropriate software, the DMTA provides a powerful tool for the study of high damping materials. The drawback to the DMTA is the high cost, this being close to \$200,000 for a complete installation. Barring purchase of the system, selected NPS students could spend several weeks at David

Taylor during their thesis quarter, conducting necessary experimentation.

IV. ENGINEERING APPLICATIONS

A. GENERAL

Selection of a particular material for an engineering application is the culmination of a long process of design, testing and evaluation. A balance must be struck between cost, mechanical properties, system interoperability and a multitude of other factors. In order to judge the usefulness of the various alloys available, a survey was conducted of the known special metals manufacturers in the United States and some overseas (see Appendix C). Results of this survey combined with a literature search formed the basis for the judgments made herein.

B. SPECIFIC ALLOY SYSTEMS

1. FeCrMo

This family of ferromagnetic damping alloys has been exploited commercially over the last 15-20 years. The material used in this research is a derivative of Vacrosil 010, produced by Vacuumschmelze of West Germany. Toshiba Corp. of Japan, developed and produced a FeCrAl alloy known as Silentalloy, which has found some use in the automobile industry. Both of these metals have excellent damping properties, in excess of 40%, which are activated at low stress levels and then drop off as strain amplitude increases. At this point, there is no precise data to

correlate normal shipboard machinery noise levels with these experimentally determined strain levels. The tensile strength (UTS) of these alloys is comparable to that of aluminum, but a severe weight penalty is incurred (three times heavier). It is quite possible to increase their strength, however, an inverse relationship exists between UTS and damping capacity. Damping is relatively insensitive to temperature change, with studies done by Toshiba indicating that damping may be unaffected up to 300° C [Ref. 18]. Finally, Schneider [Ref. 19] found that damping was destroyed by cold work in excess of 5%.

Little work has been completed on actual use of FeCrAl type alloys in military applications. The most prominent work to date was done by ManLabs, Inc., in which a 1/6 scale model of a M-113 armored personnel carrier (APC), normally made from aluminum alloys, was fabricated from a derivative of Silentalloy. Dynamic testing was completed at various speeds with maximum noise reductions realized at 50 mph, (noise reductions averaged six decibels throughout the sound spectrum). In addition, a scale model of a torpedo propeller was fabricated from a FeCo alloy and tested, with similarly successful results.

Currently work is underway at Naval Undersea Systems Center (NUSC), Newport, R.I. and at David Taylor using the FeCrAl alloys. Initial results are promising and could lead to more widespread naval applications.

2. TiNi

Nitinol was originally developed by the Naval Ordnance Laboratory in the early 1960's. It is a shape memory alloy and has found extensive applications as a fastener and for use as thermal actuators. It is widely available both in the U.S. and Japan and comes in a variety of wire forms. Nitinol is extremely corrosion resistant and has many bio-medical applications. A primary disadvantage is the high cost of titanium, which would appear to rule out its use for any widespread shipboard application. In addition, Nitinol can only be welded to itself or to titanium, by use of the electron beam method. Welds are susceptible to early fatigue failure in the heat affected zone [Ref. 20]. Cronauer found that for the alloy he examined (with the martensitic transformation occurring between 45-80° C) approximately half the damping was lost by 65° C, with complete elimination of high damping occurring at 85° C.

Currently, work is being conducted on the use of Nitinol in damping of aerospace structures by Boeing Corp. Nagaya [Ref. 21] described a method for avoiding the critical speeds of a rotating shaft by using the shape memory properties of Nitinol to change the stiffness of the supports. This idea has obvious applications to reducing noise levels of many centrifugal feed and coolant pumps.

3. CuMn

Two commercially developed variants of the CuMn alloy system, Incramute and Sonoston, have been extensively investigated to determine their noise reduction potential. Incramute was originally developed by the International Copper Research Association (INCRA) in the 1960's and INCRA subsequently funded several research studies of potential applications to vibration and noise control. The final report of INCRA project 220 [Ref. 22] concluded that achieving damping equivalent to an elastomer-steel composite could only be done at three times the cost of the composite. Sound transmission through piping, valves and enclosures were also examined, but no significant advantage in using Incramute vice normal structural materials was found. Significant reductions in noise levels were predicted for gear type applications involving low power transmission and service temperatures below 150° F (due to low martensitic transformation temperatures). The report concluded that "for applications where external systems damping is not practical, operating temperatures are not too high and structural strength per pound of metal is not a constraint, Incramute offers promise for application to reduction of noise and vibration in machinery--particularly when impact excitation is involved."

One of the primary disadvantages cited for Incramute in the past has been the reputed effect of room temperature

aging, which can reduce damping by as much as 85% after 100 hours. Recent work done by Ross and Van Aken [Ref. 23] at the University of Michigan suggests that this loss of damping is a result of pinning of twin-domain boundaries by interstitial solute atoms. Application of a large enough stress results in a so called "breakaway effect," which will unpin the boundaries and increase damping again. In addition, Ross demonstrated that small additions of erbium increased the damping capacity of Incramute by as much as 188%, as well as dramatically reducing the room temperature aging effects. This is attributed to preferential tying up of interstitials by erbium-rich dispersoids, leaving the boundaries unpinned and free to absorb energy.

The other major commercially known CuMn alloy is Sonoston which was developed by Stone Manganese Marine Limited of England in the mid-1960's. Sonoston was developed specifically as a casting alloy and its primary use has been for ship and submarine propellers. The Royal Navy has had over 25 years experience with the use of these propellers and appears to be satisfied with their performance. Like Incramute, the damping capacity of Sonoston begins to decrease above room temperature, falling to near zero at about 90° C. A major obstacle to U.S. Navy exploitation of this alloy has been uncertainty over the stress corrosion cracking resistance in seawater. While smaller test specimens have demonstrated low resistance to

attack, practical experience indicates that these propellers can be effectively operated in a marine environment, including those which have undergone weld repair. Further information on the mechanical properties of Sonoston is contained in SMM technical brief no. 15, which is duplicated in Appendix B.

4. CuZnAl

Proteus N.V. of Belgium and Raychem Corp. are two leading producers of CuZnAl alloys. They are available in a variety of bar and wire forms, as well as sheets. The only known application of CuZnAl for damping purposes was its utilization in shielding of a spectrometer in a satellite during launching [Ref. 11]. Mechanical properties of the alloy are similar to those of CuAlNi, however CuZnAl is easier to machine and some cold working is possible. Stress corrosion resistance is poor.

5. CuAlNi

To date there have been no known damping applications of CuAlNi. Developed in the early 1980's, this shape memory alloy is distinguished by achievable martensitic transformation temperatures approaching 200° C and consequently an increased temperature range for effective damping. The major obstacle to commercial exploitation of this alloy has been its inherently brittle nature. The key to improving these properties has been by means of grain size refinement. Typically, grain refinement has been

accomplished by either alloy additions or by powder metallurgy. Both titanium and zirconium have been shown to be effective grain refining elements [Ref. 24]. Mukunthan suggests that lowering Al content limits oxygen segregation at grain boundaries and leads to improved ductility and fatigue life [Ref. 25]. Husain [Ref. 26] showed that adding small amounts of boron and aging the alloy was an effective means of improving the fracture behavior. Sure indicates that as grain size is reduced and fracture behavior improved, the fatigue life is greatly improved [Ref. 27]. Powder metallurgy techniques which utilize a stable Alumina surface film which results in fragmenting into extremely fine particles during hot working have been successfully used by Proteus N.V. Their product is claimed to have an ultimate tensile strength of up to 1200 Mpa, fatigue limit of 350 Mpa, 6% ductility, transformation temperature of up to 170° C and a SDC of 10% [Ref. 28]. It should be noted that many successful applications of CuAlNi's shape memory properties have been made, ranging from fire protection systems to green house openers.

Clearly, the full potential of the CuAlNi alloy system has not been achieved, yet even at this early stage of its development it holds great promise for use in damping applications. Improving the above mentioned mechanical properties while maintaining the higher transformation

temperatures remains the key for future widespread commercial and military applications of this alloy.

6. Other Alloy Systems

Recent work by Wong [Ref. 29] has shown that high damping aluminum alloys can be produced by addition of indium. The higher damping is associated with the production of viscoelastic second phase particles. While this work is still preliminary in nature, it may open up a new area of damping research.

Another alloy which has been more extensively tested and its performance documented is austempered ductile iron (ADI). ADI has a damping capacity equivalent to that of gray cast iron, the best of the non-high damping materials. Several of its properties make it very attractive for gear type applications, including extremely good wear resistance and excellent toughness, while having double the strength of conventional ductile irons [Ref. 30]. Current commercial applications include use of ADI for a timing gear in a Cummins diesel engine and for a crankshaft in a Ford turbocharged engine. In both cases, unit costs are lower and expected life of the parts is higher than that of the non-damping material it replaced. There are immediate applications for ADI in marine diesel plants. Both the LST-1179 and LSD-41 class are diesel main propulsion and future amphibious shipping is expected to follow this trend. With the advent of the LCAC and V-22, the extension of the

amphibious operating area (AOA) out to 50 miles or more will become a reality and detectability will be a major consideration. Now is the time to begin taking steps to quiet the "gator navy," as well as the rest of the force.

V. CONCLUSIONS AND RECOMMENDATIONS

A. CONCLUSIONS

1. Equipment

Using the present equipment setup, testing at higher strain levels leads to component failure and non-linearity of results. In order to obtain usable data in this range, it is necessary to resume use of the torsional pendulum technique, coupled with a digital instrumentation package. Within the linear range the resonant dwell apparatus may still be used. A commercial environmental chamber should be obtained which can be easily modified to accommodate use of an optical measurement system. Use of the DMTA on a time-share basis with David Taylor should be considered.

2. Alloy Systems

In considering possible shipboard applications of high damping alloys, their use should not be limited to one-for-one replacement items but rather should be incorporated in the earliest design stages of entire systems. These alloys should not be viewed as competing with the various visco-elastic treatments, but rather as being complementary to them. Of the presently available materials, the ferromagnetic damping alloys seem most suitable for direct application. The copper based shape memory alloys show great promise and applications utilizing both their shape memory effect and damping should be considered in the design

of systems. Austempered ductile iron has the potential for extensive use in diesel propulsion plants. In order to evaluate these materials properly, an engineering test ship should be designated, like the very successful USS Norton Sound (AVTM-1) and USS Glover (AGFF-1).

Research continues into other promising high damping alloys. Dr. Schetky of Memory Metals, Inc., recommends seeking matrix strengthening by precipitation to achieve thermoelastic martensites in the FeNi system. This alloy would combine the best properties of the shape memory metals and the advantages of a ferrous based system, namely low cost and good mechanical properties.

B. RECOMMENDATIONS

The following recommendations are provided:

1. Continue work on the CuZnAl and CuAlNi alloy systems. Determine the optimum high damping condition for both systems and fully investigate other mechanical properties in that condition.
2. Find the correlation between shipboard machinery noise levels and strain, as determined in this research.
3. Conduct a survey at the classified level of noise signatures associated with components made of high damping alloys installed onboard ships and submarines using fleet ASW assets.

APPENDIX A

PROCEDURE FOR READING STRAIN MEASUREMENTS

Prior to using a strain gage for the measurement of damping and strain amplitude, it must be calibrated and a static measurement should be conducted. Step by step procedures can be found in the BAM-1 instruction manual on pages 6-8.

Once the BAM-1 has been initially adjusted in accordance with paragraphs 2.6-2.13 of the instruction manual, the gage factor is used to determine the proper calibration number setting, using Equation 2-1 of the manual. All gages used in the experiment had a gage factor of 2.12. The desired full scale strain reading on the BAM-1 was 1000 microstrain. Therefore, the calibration number was determined to be:

$$1000(2.12)*1/400 = 5.3$$

Rounding down, the BAM-1 CAL SET knob is set to 5 and the shunt calibration is now determined by Equation 2-3:

$$(400)*(5)/(2.12)*(1) = 943$$

Using paragraph 2.18 of the manual as a guide, this number is now used to prepare the BAM-1 for a static

measurement. Connect the strain gage to the BAM-1, unplug all outputs, and balance the unit. Now deflect the beam half an inch and read the BAM-1 directly to determine microstrain. This is a ballpark figure used to check dynamic measurements from the Signal Analyzer.

Prior to conducting dynamic measurements, the BAM-1 is connected to the multimeter and then to the signal analyzer. With the BAM-1 CAL switch in the + position, adjust the GAIN knob until the multimeter reads .0943 volts. Now turn on the Signal Analyzer and go to page 5, Y CALIB PARAMETERS. Set VREF at .001, EU (@ VREF) at 100 and all other categories at 0. The apparatus is now ready for operation, and strain may be read directly from setup page 3, DISPLAY SELECTIONS.

APPENDIX B

TABLES OF MATERIAL PROPERTIES

Contained in Appendix B are a compilation of material properties of some of the high damping alloys discussed in this document. The original figure and table numbers have been reproduced and referenced appropriately.

TABLE Ia. Properties of Shape Memory Alloys in Heat-Treated Condition

ITEM	UNIT	Ni-Ti	Cu-Zn-Al	Cu-Al-Ni
Melting point	°C	1240-1310	950-1020	1000-1050
Density	kg/m ³	8400-8500	7800-8000	7100-7200
Electrical Resistivity	10 ⁻⁶ m	0.5-1.10	0.07-0.12	0.1 - 0.14
Thermal conductivity	W/m°C	(10-118)	120 (bij 20°C)	75
Thermal expansion Coefficient	10 ⁻⁶ °C ⁻¹	10 (5)/8.6 (Mart.)	16-18 (Mart.)	16-18 (Mart.)
Specific heat	J (kg°C) ⁻¹	470 (-620)	390	(400-) 480
Thermo-electric Power	10 ⁻⁶ V.°C ⁻¹	9-13 (mart.)	-	-
Transformation Enthalpy	J/kg	5-8 (H)	7000-9000	7000-9000
E-modulus	GPa	98	70-100	80-100
Yield Stress (0.2)	MPa	150-300 (Mart.)	150-300	150-300
UTS (mart.)	MPa	800-1100	700-800	1000-1200
Elongation at Fracture (mart.)	%	40-50	10-15	8-10
Fatigue Strength M=10 ⁶	MPa	350	270	350
Grain Size	10 ⁻⁶ m	50-100	50-100	25-60
Transformation Temperature Range	°C	-100° to +120°C	-200° to +120°C	-200° to +170°C
Hysteresis (A ₁ -A _c)	°C	30 -	10-20	20-30
Max. one way memory	%	8	5	6
Max. two way memory	%	6	1	1.2
N = 102		2	0.8	0.8
N = 105		0.5	0.5	0.5
N = 107		400	160-200	300
Overheating temperature	°C	15	30	10
Damping capacity at strain amplitude of 10 ⁻³	SDC-%			
Max. pseudol. tensile strain	%	10	10	10
- single crystal	%	4	2	2
- poly crystal	%			
Corrosion Resistance		Excellent	Fair	Good
Biological Compatibility		Excellent	Bad	Bad

[Ref. 11]

		<u>"Incramate"¹</u>	<u>"55-Nitinol"</u>	<u>Mild Steel²</u>	<u>Brass³</u>
SDC	% @ 5000 PSI	40	40	4	0.2
UTS	KSI	85	125 ⁵	70	47
YS	KSI	45	25 ⁵	50	15
Ductility	% elong.	30	60 ⁵	30	50
Modulus, E	PSI x 10 ⁶	12	12.5 ⁶	30	16
Density	g/cc	7.49	6.45		8.53
Melting point	°F(°C)	(914)	2390 (1310)	2775	1750
Thermal expansion ⁴	α μ -in/in/°C	22.5	10.4	8.4	11.1
Fatigue strength	KSI for 10 ⁶ cycles	20	70 ⁷		14
Hardness	R _B (BHN)		90	(140)	65
Thermal conductivity	K(BTU/ft/hr/°F)			27	70
Electrical resistivity	μ -ohm-cm		80		6.2
Electrical conductivity	% IACS@70°F				28
Specific heat	BTU/lb/°F@70°F			.10	.09
Magnetic permeability			< 1		

1: in optimum damping condition

2: normalized 1025 steel

3: 70-30 (cartridge) brass, annealed

4: mean coefficient, 25°C-1000°C

5: exact values dependent of test temperature relative to transition temperatures

6: of high-temperature phase

7: 10⁷ cycles

[Ref. 31]

VACROSIL 010
Manufactured by Vakuumschmelze GMBH, West Germany

Composition
(weight percent)

Properties

Fe	Balance	Tensile Strength (ksi)	- 50
Cr	12	Yield Strength (ksi)	- 46
Al	3	Elongation (%)	- 22
		Impact Engery (ft-lb)	-
		Young's Modulus (10^6 psi)	- 25

Heat Treatment: Annealed 1100° C
 See Figures 1 and 4 for other heat treatments

Damping Mechanism: Magnetomechanical Hysteresis

Damping Capacity: 60% for stress amplitude 1.45×10^{-9} psi for heat treatment 1 - See Figures 1, 2, 3 and 4

Temperature Range: Can be used up to 300° C

Comments:

Abbreviations: P = Specific damping capacity

[Ref. 18]

Table 1: Physical properties of FeCr based alloys after annealing at 1100°C/1 h. Vacrosil 010

	HV ₅	R _m N/mm ²	R _{p0.2} N/mm ²	A _{1.50} %	E 10 ³ /mm ²	R _c N/cm	2 s(max)
Fe-10Cr	114	-	-	-	206	1.2	13
Fe-12Cr	123	268	157	26	177	0.28	39
Fe-14Cr	132	287	149	20	176	0.33	35
Fe-16Cr	137	310	144	24	173	0.33	35
Fe-12Cr-2.5Mo	160	329	257	10	185	0.64	37
Fe-12Cr-2.5Mo-2.5Ti	185	402	276	5	188	3.3	11
Fe-12Cr-2.5Mo-1Cu	201	430	319	18	180	0.63	42
Fe-16Cr-2.5Ti	182	450	288	8	193	2.88	14
Fe-16Cr-2.5Ti-2.5Mo	201	392	346	2	224	4.7	44
Fe-16Cr-2.5Ti-1Cu	210	460	388	4	195	2.98	15
VACROSIL® 010 (Fe-12Cr-3Al)	183	394	306	22	175	0.3	60

® = registered trade mark

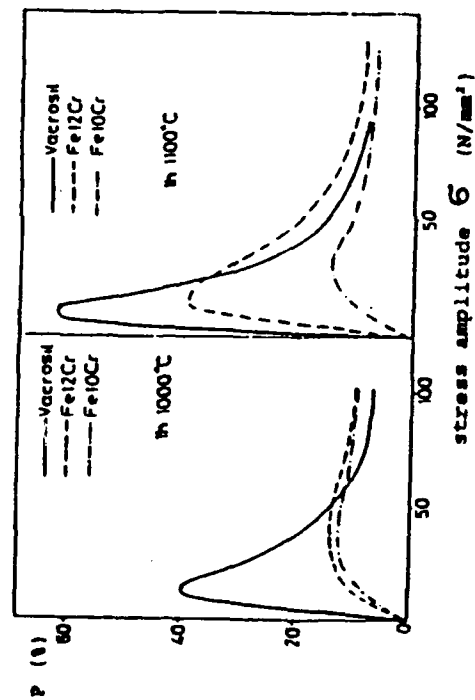


Fig. 1 : Damping capacity of various Fe-Cr alloys heat treated at 1000°C and 1100°C.

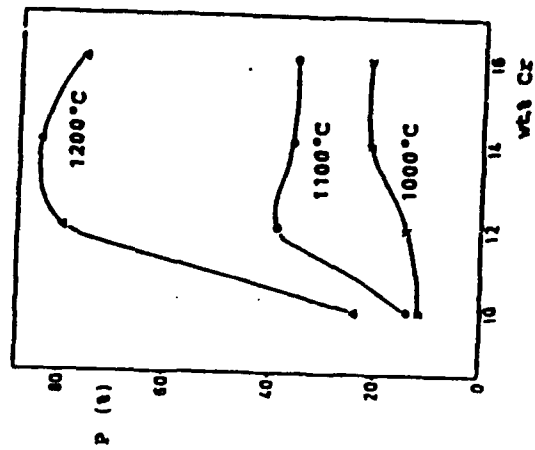


Fig. 2 : Maximum damping capacity vs. Cr content.

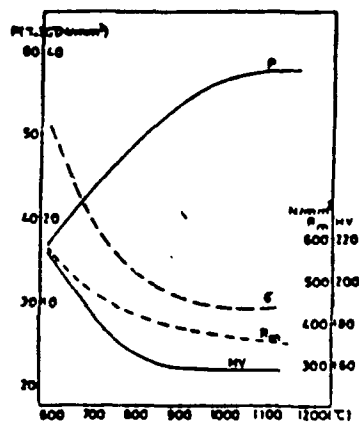


Fig. 3 : Maximum damping capacity (P) and the corresponding stress amplitude (σ), tensile strength (R_m) and hardness (HV) as a function of annealing temperature (annealing time 1 h)

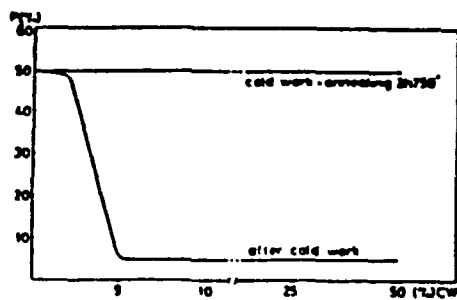


Fig. 4 : Effect of cold work on the damping capacity

INCRAMUTE I

Composition (weight percent)		Properties	
Cu	55 - 58	Tensile Strength (ksi)	- 81-85
Mn	40 - 43	Yield Strength (ksi)	- 36-45
Al	2	Elongation (%)	- 34-27
		Impact Energy (ft-lb)	-
		Young's Modulus (10^6 psi)	- 12-14

Heat Treatment:

Damping Mechanism: Magnetomechanical hysteresis plus metastable miscibility gap in fcc phase

Damping Capacity: See Figures 1, 2, 12, 13, 14, 18, 19, 20, 21 and 82

	Loss Factor
At 68° F 1 ksi	17×10^{-3}
5 ksi	40×10^{-3}
10 ksi	60×10^{-3}

SDC = 40% at a surface shear stress = 78 ksi

Temperature Range: Below 110° C
This alloy is fct below antiferromagnetic N'eel temperature

Comments:

Abbreviations: Q^{-1} = Loss factor

SDC = Specific damping capacity

[Ref. 1B]

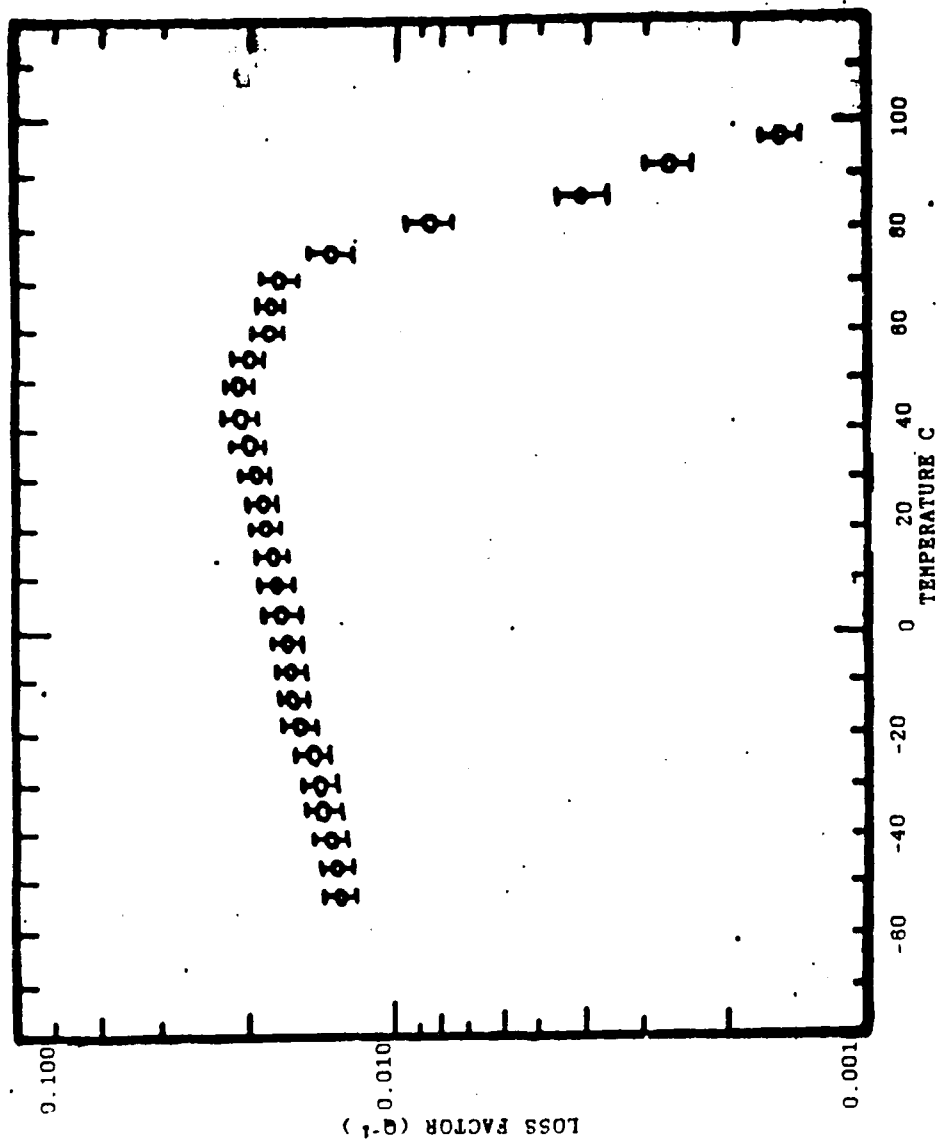


Figure 82. Loss Factor vs. Temperature for a Sample of Incramute I (nominal composition 55 w/o Cu-43 w/o Mn-2 w/o Al) heat treated for maximum damping characteristics and measured at 180-220 hertz at a peak stress of 2000 psi. The dynamical Youngs Modulus varies from 12.5 million psi at 1000 C to 15.5 million at -600 C.

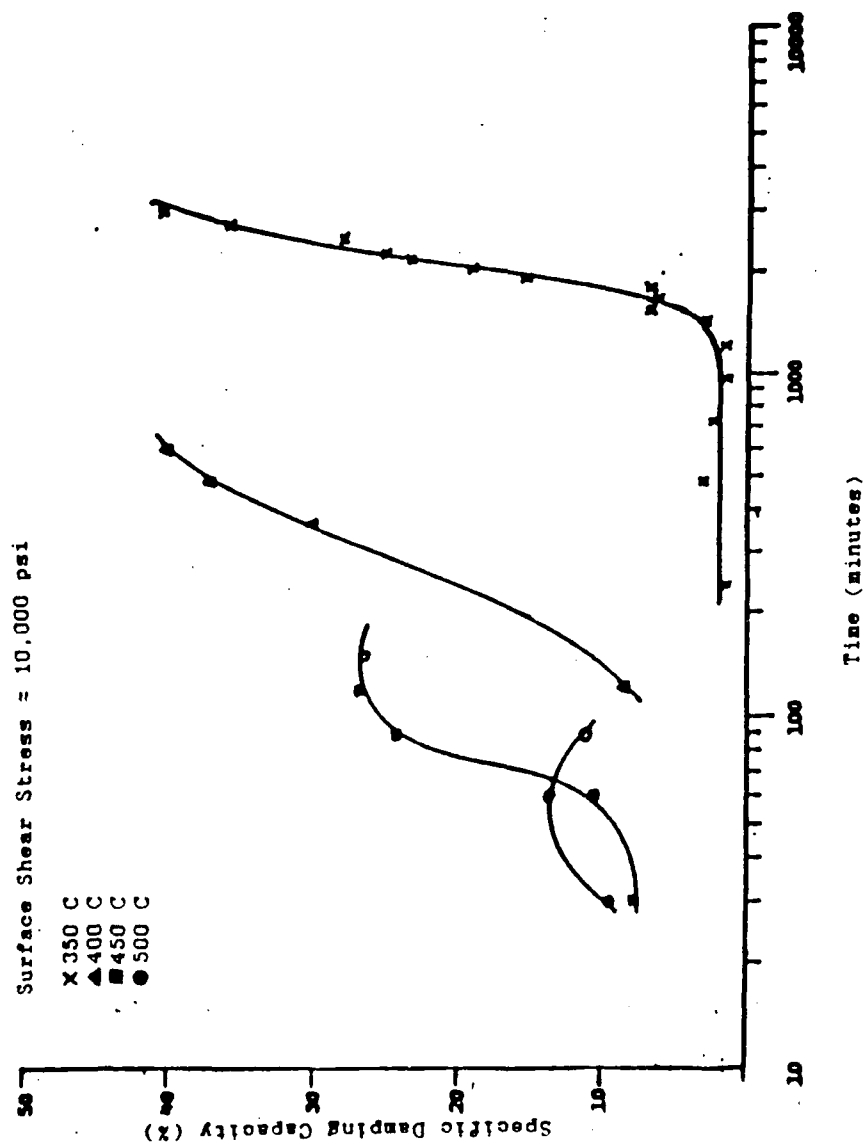


Figure 20. Effect of Aging Time on Damping Capacity When Measured at 10,000 psi Surface Shear Stress

INCRAMUTE I

Figure 1: Effect of peak applied stress on the room temperature loss factor of INCRAMUTE I which has been solution annealed, water quenched and aged at 400°C for the indicated times.

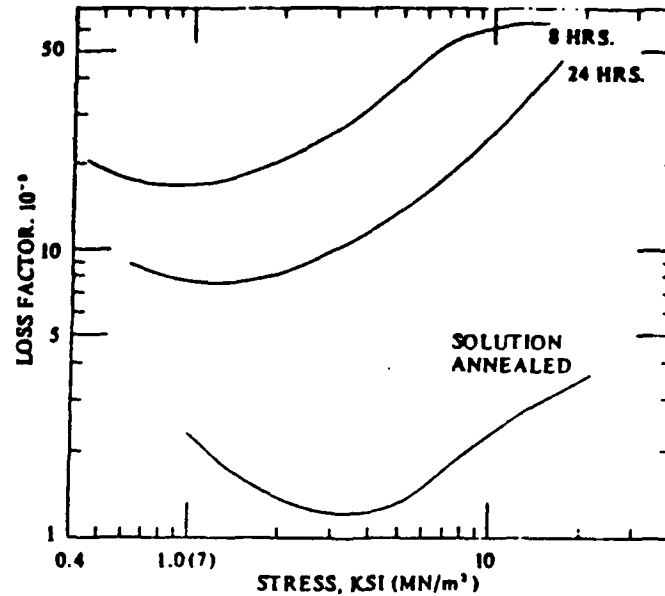


Figure 2: Effect of test temperature on the loss factor-peak applied stress curves for INCRAMUTE I after aging at 400°C. 24 hours.

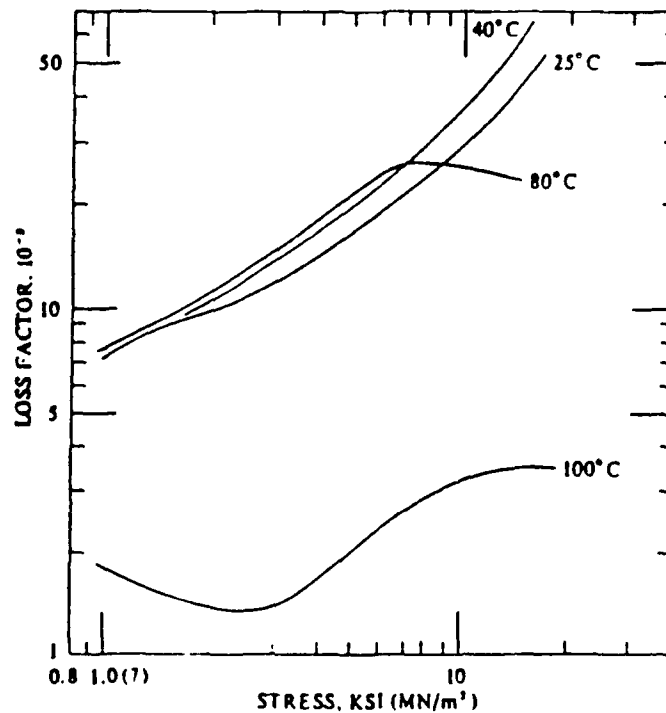


Figure 14: Table of SDC data for "Ingramite" aged at 500°C

Time of Aging Temperatures hours	Surface Shear stress, PSI		
	1000	5000	10,000
0.5	6%	7.85%	8.75%
1.0	7.15%	6.9%	13.7%
1.5	5.58%	6.65%	11.2%

INCRAMUTE II

Composition (weight percent)		Properties	
Mn	40.0 - 48.0	Tensile Strength (ksi)	- 80*, 90**
Al	1.40 - 2.25	Yield Strength (ksi)	- 36*, 58**
Sn	1.50 - 2.50	Elongation (%)	- 34*, 20**
Cu	Balance	Impact Energy (ft-lb)	-
		Young's Modulus (10^6 psi)	- 13*

Heat Treatment:

Damping Mechanism: Magnetomechanical hysteresis plus metastable miscibility gap in fcc phase

Damping Capacity: $Q^{-1} = 3.5 \times 10^{-2}$ at 1 ksi and 68° F
 $Q^{-1} = 1.1 \times 10^{-2}$ at 10 ksi and 68° F
 See Figures 3 and 4

Temperature Range: 200°-300° F or below

Comments:

Abbreviations: * = Solution Treated
 ** = Aged
 Q^{-1} = Loss factor

[Ref. 18]

Figure 3: Effect of peak applied stress on the room temperature loss factor of INCRAMUTE II which has been solution annealed, water quenched and aged at 400°C for 24 hours.

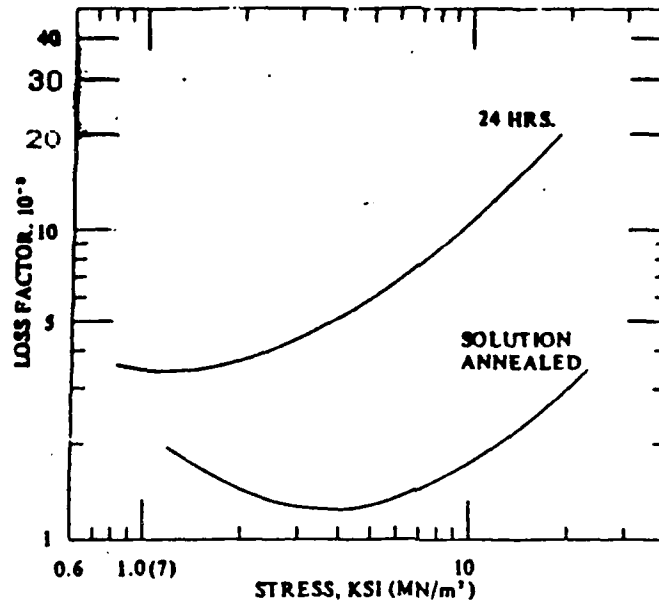


Figure 4: Effect of test temperature on the loss factor-peak applied stress curve for INCRAMUTE II after aging at 400°C-24 hours.

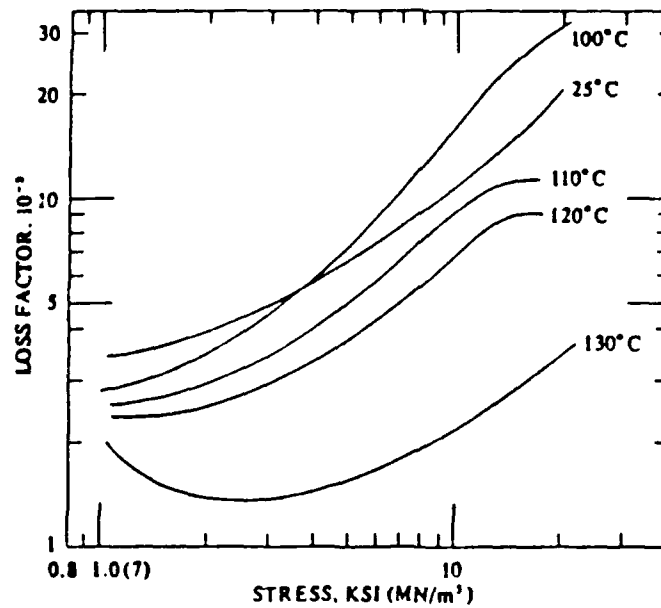
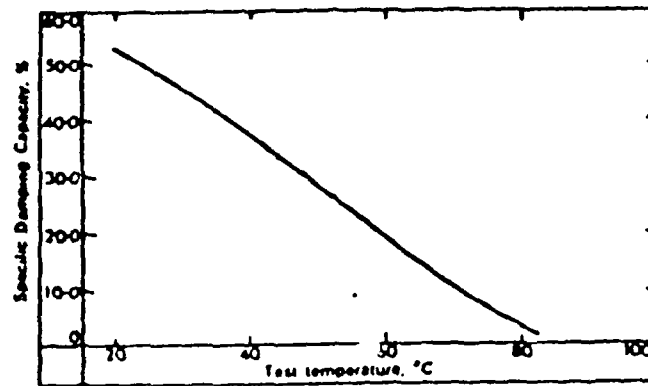


Fig. 15. Effect of temperature on damping capacity



AUSTEMPERED DUCTILE IRON
grade one

	Composition (weight percent)	Properties
Fe	Balance	Tensile Strength (ksi) - 125
C	3.1 - 3.8	Yield Strength (ksi) - 80
Mn	^{0.02} 0.2 - 0.5	Elongation (%) - 10
Si	2 - 2.8	Impact Energy (ft-lb) - 75 unnotched
Ni	1.0 - 1.5	Young's Modulus (10^6 psi) - 20
S	0.02 max	Density at room temperatures 0.27 lb/in^3
Mo	0.1 - 0.4	
Mg	0.03 - 0.05	
P	.03 max	

Heat Treatment: 1700°F for 1.5 Hr, quench to 460°F where it is held for 2 Hr.

Damping Mechanism: Dislocation movement in graphite nodules

Damping Capacity: $Q^{-1} = 1 \times 10^{-2}$ - loss factor

Comments: casting size limitations 6 inches thickness which is sufficient for controllable pitch propellers but not aircraft carriers.

[Ref. 18]

SONOSTON

Composition (weight percent)		Properties	
Mn	54.25	Tensile Strength (ksi)	- 78-90
Cu	37.0	Yield Strength (ksi)	- 35-45
Al	4.25	Elongation (%)	- 20-40*
Fe	3.0		15-35**
Ni	1.50	Impact Energy (ft-lb)	- 20-40*
			10-30**
		Young's Modulus (10 ⁶ psi)	- 10.5-12

Heat Treatment:

Damping Mechanism: Martensitic transformation

Damping Capacity: SDC = 10-30%
SDC = 12% at 1000 psi
SDC = 14% at 2500 psi
SDC = 19% at 5000 psi
See Figure 16

Temperature Range: Below 50°-60° C

Comments: SCC in seawater, fatigue, corrosion fatigue, SCC data, and foundry experience are available.

Abbreviations: *As cast
**Stress relieved
SCC = Stress corrosion cracking
SDC = Standard damping capacity

[Ref. 18]



Published by
STONE MANGANESE MARINE LIMITED

No. 15: Sonoston high damping capacity alloy

(This Publication replaces SMM Technical Brief No. 7)

Introduction

Materials of high damping capacity are invaluable for use where freedom from vibration and noise is at a premium, and where structural damping cannot be employed to that end. Sonoston is a relatively new alloy based on manganese which combines a high damping capacity with mechanical properties which make it suitable for engineering purposes.

Its specific damping capacity can be varied, but is generally of the order of about 20% at high strains. This is about twice the damping capacity of grey cast iron, and more than 20 times greater than most other engineering alloys.

Its greatest use has been for marine propellers in which it is difficult to effect damping by other means.

Sonoston is protected by British Patent 984,870 and by its equivalent in other countries.

Mechanical Properties

The mechanical properties of Sonoston are detailed in the table at the end of the Brief from which it will

be seen that they are comparable with those of manganese bronze.

The stress-strain curve shows marked strain hysteresis on unloading, the magnitude of which is greater, the greater the damping capacity of the alloy.

Proof stress, tensile strength and damping capacity are maintained in heavy sections, although ductility is reduced to some extent.

Charpy tests showed a gradual fall in energy as the test temperature was reduced from +100°C to -180°C, although even at the lowest temperature the fractures were ductile.

Although heat treatment is not normally required, thin section sand castings or die castings may not have adequate damping capacity, but this can be raised to satisfactory levels by means of a simple heat treatment of 4 hours at 400°C or $\frac{1}{2}$ hour at 450°C, followed by slow cooling. The same treatment is recommended for the stress relief of complex castings, but it should be noted that the treatment reduces elongation by some 5-10 per cent and the Izod value by about 10 J.

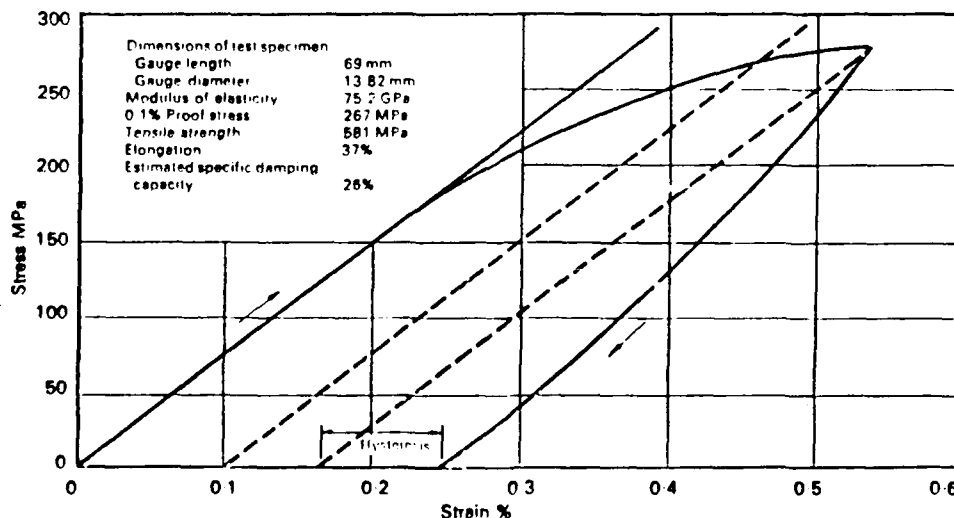


Fig 1. Typical tensile stress—strain curve for Sonoston alloy

Physical Properties

The damping behaviour of Sonoston is little affected by frequency but is affected by the stress level. Damping capacity falls above room temperature and is practically zero at about 90 °C.

Other physical properties are detailed in the table at the end of this Brief. Sonoston has a high electrical resistance and a low thermal conductivity.

Fatigue Resistance

The fatigue strength of specimens from small castings tested in air is 140 MPa at 100 megacycles and in 3% sodium chloride 75 MPa.

The effect of section size on the corrosion fatigue strength of Sonoston appears to be less than is the case with other propeller alloys. Nevertheless it can be expected that material from very thick sections will have corrosion fatigue strengths lower than those of small castings.

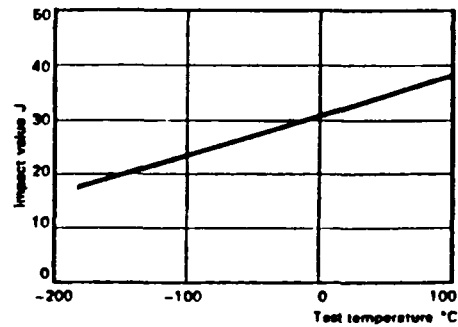


Fig. 2. Effect of temperature on the Charpy ('V' notch) impact resistance of Sonoston.

Corrosion Resistance

The alloy is not heavily oxidised in air at temperatures up to 500 °C and can safely be heat-treated at higher temperatures.

Corrosion in sea water takes place by a process similar to the dezincification of brasses with little or no surface loss even with very high water velocities.

Sonoston is anodic to copper-base alloys and stainless steels. On the other hand it is cathodic to mild steel, aluminium alloys and zinc by any of which it can be successfully protected against corrosion, even under conditions of severe impingement.

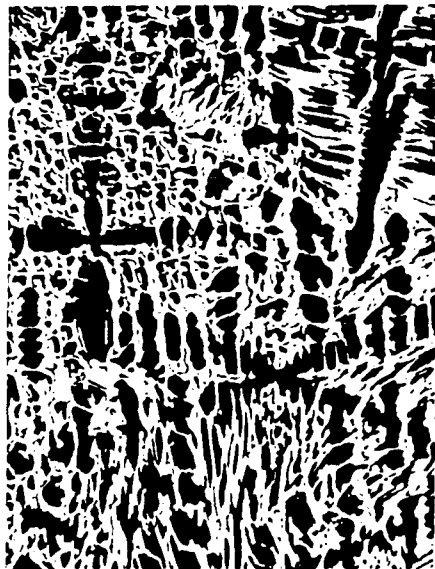


Fig. 3. Microstructure of Sonoston etched in ammonium persulphate to show the cored solid solution with the hard beta phase in between the dendrite arms. X 150



Fig. 4. As in Fig. 3 but at higher magnification and etched in mixed chromic and nitric acids to show more clearly the beta phase containing dark particles of a third phase. X 600

Stress Corrosion

It has been found that Sonoston is susceptible to stress corrosion cracking in 3 per cent sodium chloride solution. However, the composition of the alloy has been selected to give the best resistance to this type of attack consistent with the other properties required of the alloy.

It has been found that the resistance to stress corrosion cracking is better in thick than thin cast sections and that cracking can be avoided by suitable cathodic protection.

It is important in this regard not to subject the alloy to rapid cooling after welding or any thermal treatment.

Cavitation Erosion Resistance

Tests using a magnetostriction device have indicated that the alloy is not as resistant to cavitation erosion as are the alloys normally used for propeller manufacture.

Metallography

The microstructure of alloys of the Sonoston type consists mainly of a heavily cored matrix of copper-gamma manganese solid solution. Aluminium in excess of about 2.5% causes formation of a beta phase (thought to be isomorphous with beta copper aluminium) which normally contains small particles of another phase. The processes responsible for the good damping capacity of Sonoston are similar to those in the binary manganese copper alloys.

Heat Treatment

Although heat treatment is not essential, thin sectioned sand castings and die castings may not have adequate damping capacity without heat treatment whilst complex castings may contain undesirable locked-in stresses. A simple heat treatment of 4 hours at 400°C or half an hour at 450°C, followed by slow cooling, serves for both these purposes and for stress relief after welding.

Prolonged heating in the range 400-750°C is undesirable as it can lead to loss of ductility, whilst heating to any temperature above 500°C and cooling rapidly lowers the damping capacity. The effects of heating between 500°C and 750°C can best be overcome by re-heating to 850°C and slowly cooling (about 100°C/hr.).

Casting Characteristics

The alloy can be melted and cast by relatively conventional techniques. Its wide freezing range of about 140°C gives it casting characteristics which are generally similar to those of tin bronzes and gunmetals.

Its casting contraction is high, varying from 1 in 30 when contraction is free, to 1 in 35 under restraint, and gives a risk of hot tearing unless care is taken to avoid severe restraint in the mould.

Machining Characteristics

Sonoston is roughly similar to stainless steel in its machining behaviour. Features which should be noted are that the alloy heats considerably on machining and that the low modulus of elasticity (similar to that of aluminium alloys) may cause bowing of thin sectioned castings if chucks are tightened too much or if excessively heavy cuts are taken.

For turning with tungsten carbide tipped tools a 6° positive rake, 6° clearance and 15° approach angle are recommended—Sandvik Grade S4 tools have been found to be particularly suitable.

Welding

The alloy can be welded successfully by the MMA, MIG or TIG processes using Superston 40 as a filler material. Stress relief heat treatment is essential, a treatment of four hours at 400°C normally being suitable.

Applications

Apart from its use for marine propellers, other potential applications can be foreseen where castings are required to have good damping capacity to suppress noise and vibration in conjunction with good strength and shock resistance.

Castings which have already been made include shock proof instrument mountings, pump cases, supports for machine tools and diesel engine parts. The alloy is not suitable however for applications where the temperature of the component exceeds about 50°C in service.

Specified Minimum Tensile Properties

0.1% proof stress	
MPa	250
kg/mm ²	25.5
Tensile strength	
MPa	540
kg/mm ²	55.0
Elongation % on 5.65 $\sqrt{S_0}$	13
Specific damping capacity %	10

Mechanical Properties

Tensile Properties	Unit	Range	Typical
0.1% proof stress	MPa kg/mm ²	250-280 25.5-28.5	270 27.5
Tensile strength	MPa kg/mm ²	540-590 55-60	565 58
Elongation, as cast	%	13-30	25
Elongation, stress relieved	%	13-30	20
Modulus of elasticity (Young's modulus)	GPa kg/cm ²	73-83 0.75-0.85 $\times 10^6$	77 0.8 $\times 10^6$
Other Properties			
Hardness, Brinell	10/3000	130-170	150
Izod impact value, as cast	J kg m kg m/cm ²	25-55 2.8-5.5 3.5-6.9	40 4.2 5.2
Izod impact value, stress relieved	J kg m kg m/cm ²	14-40 1.4-4.2 1.7-5.2	27 2.8 3.5

Physical Properties (typical values)

Melting Range	940-1080 °C
Specific gravity	7.1
Linear coefficient of thermal expansion, 20-100 °C	16.5 $\times 10^{-6}$ /°C
Estimated specific damping capacity	10-30%
Electrical resistivity	120 microhm/cm ² /cm
Electrical conductivity	1.5% IACS
Magnetic permeability	1.15-1.40
Potential against calomel electrode in 3% sodium chloride solution	-0.7 volt

The descriptions, illustrations, dimensions, performance figures and other particulars contained in this leaflet are given in good faith but are not intended to and do not constitute any guarantee or warranty given by the company, nor do they form part of any contract.

STONE MANGANESE MARINE LIMITED, RIVERSIDE HOUSE, ANCHOR & HOPE LANE, LONDON SE7 7SZ

Telephone: 01-858 8171

Telegraph: SHIPSPROP, LONDON, SE 7

Telex: 897359

A member of the Stone-Platt Group

Printed by E. G. Barryman & Sons Limited, 84 Blackheath Road, London SE10 8DB, June 1977

APPENDIX C

LIST OF ADDRESSEES

1. Dr. Ian Ritchie
Atomic Energy of Canada, Limited
Whiteshell Nuclear Research Establishment
Pinawa, Manitoba ROE 1L0 Canada
2. Steve Robinson
Boeing Aerospace Company
P.O. Box 3999
Seattle, Washington 98124-2499
(206)-773-1894
3. Catherine Wong, Code 2812
David Taylor Naval Ship R&D Center
Annapolis, Maryland 21402
(301)-267-2835
4. Dr. Dale Peters
International Copper Research Association
708 Third Avenue
New York, New York 10017
(212)-697-9355
5. Dr. Jan Van Humbeeck
Katholieke Universiteit Leuven
Departement Metaalkunde en Toegepaste Materiaalkunde
de Croylaan 2
B-3030 Heverlee, Belgium
6. Prof. Sugimoto
Dep. of Met., Faculty of Eng.
Kansai University
3-35, 3-chome, Yamatecho
Suita 564, Japan
7. Dr. L. McDonald Schetky
Memory Metals, Inc.
83 Keeler Avenue
Norwalk, Connecticut 06854
(203)-853-9777

8. Dr. Yoshiharu Mae
Mitsubishi Metal Corporation
Central Research Institute
1-297 Kitabukuro-cho, Omiya, Saitama 330, Japan
(0486)-41-5111
9. Dr. David Goldstein, Code R-32
Naval Surface Warfare Center
New Hampshire Avenue
Silver Spring, Maryland 20903-5000
(301)-394-2468
10. Pierre Corriveau, Code 8215
Naval Undersea Systems Center
Newport, Rhode Island 02841
(401)-841-2044
11. W. Van Moorlegghem
Proteus N.V.
Stasegemsesteenweg 110E
B-8500 KORTRIJK, Belgium
32-56-20-23-90
12. Dr. Tom Duerig
Raychem Corporation
300 Constitution Drive
Menlo Park, California 94025-1164
(415)-361-2778
13. Dr. Darel E. Hodgson
Shape Memory Applications, Inc.
285 Sobrante Way, Suite E
Sunnyvale, California 94086
(408)-730-5633
14. A. Tuffrey
Stone Manganese Marine Limited
Dock Road
Birkenhead, Merseyside L41 1DT
(051)-652-2372
15. Dr. Minoru Ichidate
Sumitomo Metal Industries, Limited
Ote Center Building
1-3 Otemachi 1-Chome
Chiyoda-ku, Tokyo, 100 Japan
(03)-282-6251

16. Dr. Kenji Adachi
Sumitomo Metal Mining Company
Central Research Laboratory
3-18-5 Nakakokubun
Ichikawa 272 Japan
(0473)-72-7221
17. Frank Sczerzenie
Special Metals Corporation
Middle Settlement Road
New Hartford, New York 13323
(315)-798-2900 ext. 2072
18. Dr. Kazuo Suzuki
Toshiba Corporation
Research and Development Center
1, Komukai Toshiba-cho
Saiwai-ku, Kawasaki 210 Japan
(044)-511-2111
19. Dr. Baker
U.S. Army Material Command
Science and Technology Center, Far East
Yokota Air Base, Tokyo
20. Chuck Hovey
U.S. Nitinol
20631 Wardell Road
Saratoga, California 95070
(408)-741-5563
21. G. Hausch
Vacuumschmelze GMBH
Gruner Weg 37
6450 Hanau, West Germany

LIST OF REFERENCES

1. Pan, Z-L., Sprungmann, K.W., Schmidt, H.K. and Ritchie, I.G., "Internal Friction in Some High Damping Alloys," Proc. ECIFUAS-5 Antwerp, July 1987.
2. Ritchie, I.G., Pan, Z-L., Sprungmann, K.W., Schmidt, H. K. and Dutton, R., "High Damping Alloys--The Metallurgist's Cure for Unwanted Vibrations," Canadian Metallurgical Quarterly, 1987.
3. Bolt, Beranek, and Newman, Inc., Cambridge, Massachusetts, "Operations Manual for the Bolt, Beranek, and Newman, Inc., Resonant Dwell Apparatus," January 1973.
4. Heil, J.P., Damping and Microstructures in Aged Cu-Mn Based Alloys, Master's Thesis, Naval Postgraduate School, Monterey, California, June 1988.
5. Cronauer, J.T., Damping Behavior of a Ti-Ni Shape Memory Alloy: Comparison with Cu-Mn-Based and Fe-Cr-Based High Damping Alloys, Master's Thesis, Naval Postgraduate School, Monterey, California, June 1987.
6. Heine, J.C., The Stress and Frequency Dependence of Material Damping in Some Engineering Alloys, Ph.D. Dissertation, Massachusetts Institute of Technology, Boston, Massachusetts, June 1966.
7. Delaey, L., Van Humbeeck, J., Chandrasekaran, M., Janssen, J., Andrade, M. and Mwamba, N., "The Cu-Zn-Al Shape Memory Alloys," Metals Forum, Vol. 4, No. 3, 1981.
8. Miyazaki, S., Otsuka, K., Sakamoto, H. and Shimizu, K., "The Fracture of Cu-Al-Ni Shape Memory Alloys," Transactions of the Japan Institute of Metals, V. 22, No. 4, 1981.
9. O'Toole, J.F. and Perkins, J., "Damping Behavior of an Fe-Cr-Mo Alloy: Strain Dependence and Heat Treatment Effects," Naval Postgraduate School Technical Report No. NPS 69-87-002, Monterey, California, December 1986.
10. Reskusich, J. and Perkins, J., "Damping Behavior of INCRAMUTE: Strain Dependence and Heat Treatment Effects," Naval Postgraduate School Technical Report No. NPS 69-87-001, Monterey, California, September 1986.

11. Aernoudt, E., Van Humbeeck, J., Delaey, L. and Van Moorlegheem, W., "Copper-Base Shape Memory Alloys: Alloys for Tomorrow," Department of Metallurgy and Materials Engineering, Katholieke Universiteit Leuven, Leuven, Belgium, p. 20.
12. Ahlers, M., "The Stabilization of Martensite in Cu-Zn-Al Alloys," Proc. ICOMAT, 1986.
13. Rappeline, P. and Perkins, J., The Microstructural Basis of Damping in High Damping Alloys, Master's Thesis, Naval Postgraduate School, Monterey, California, September 1989.
14. Le May, A. and Van Neste, A., "Influence of Cold Work on Magnetomechanical Damping in Nickel," Scripta Metallurgica, V. 8, pp. 1369-1372, 1974.
15. Dew, D.D., Strain Dependent Damping Characteristics of a High Damping Manganese-Copper Alloy, Master's Thesis, Naval Postgraduate School, Monterey, California, September 1986.
16. Bureau of Mines Report of Investigations 8774, A Digital Instrumentation Package for an Improved Torsion Pendulum, by R.W. Nash and A.E. Schwaneke, 1983.
17. Army Materials and Mechanics Research Center Report 77-9, Noise Abatement and Internal Vibrational Absorption in Potential Structural Materials, by L. Kaufman, S.A. Kulin and P.P. Neshe, pp. 13-20, February 1977.
18. David W. Taylor Naval Ship Research and Development Center SME-84-149, Compilation of Published Damping Data, by C.R. Wong and R.O. Hardies, pp. A56-A67, February 1985.
19. Schneider, W., Schrey, P., Hausch, G. and Torok, E., "Damping Capacity of Fe-Cr and Fe-Cr Based High Damping Alloys," Journal de Physique, No. 10, V. 42, pp. C5-635-C5-639, October 1981.
20. Johnson, A. David, TiNi Alloy Company to LCDR Kenneth P. Roey, Naval Postgraduate School, 25 May 1989.
21. Nagaya, K., Takeda, S., Tsukui, Y. and Kumaide, T., "Active Control Method for Passing Through Critical Speeds of Rotating Shafts by Changing Stiffnesses of the Supports with Use of Memory Metals," Journal of Sound and Vibration, 113(2), pp.307-315, 1987.

22. Wyle Laboratories Final Report INCRA Project 220, Study of Noise and Vibration Control Applications of Incramute High Damping Alloy, by Rex Sinclair, pp. 66-69, April 1974.
23. Ross, Blake A., "The Effect of Erbium Additions on the Damping Capacity and Room Temperature Aging Behavior of Incramute," Department of Materials Science and Engineering, University of Michigan, Ann Arbor, Michigan, pp. 25-30, 7 June 1989.
24. Zhongguo, W. and Dazhi, Y., "The Grain Growth Behavior of CuZnAl Alloys and the Effects of Zr and Ti Additions," Department of Materials Engineering, Dalian University of Technology, Dalian, P.R. China, p. 5.
25. Mukunthan, K. and Brown, L.C., "Preparation and Properties of Fine Grain B-CuAlNi Strain-Memory Alloys," Metallurgical Transactions A, pp. 2921-2928, Vol. 19A, December 1988.
26. Husain, S.W., Ahmed, M., Hashmi, F.H. and Khan, A.Q., "Change in Fracture Behavior on Aging of Rapidly Solidified Cu-Al-Ni Shape Memory Alloys," Dr. A.Q. Khan Research Laboratories, Rawalpindi, Pakistan, p. 1.
27. Sure, G.N. and Brown, L.C., "The Fatigue Properties of Grain Refined B-Cu Al Ni Strain-Memory Alloys," Department of Metallurgical Engineering, University of British Columbia, Vancouver, B.C., pp. 2-3.
28. Manufacturers Advertising Brochure, Proteus N.V., Shape Memory Alloys, Stasegemsesteenweg 110E, B 8500 Kortrijk, Belgium.
29. Wong, C.R., Van Aken, D.C. and Diehm, O., "Damping Capacity of Aluminum 6061-Indium Alloys," David Taylor Research Center, Physical Metallurgy Branch, Code 2182, Annapolis, Maryland.
30. Forrest, R.D., "Austempered Ductile Iron for Both Strength and Toughness," Machine Design, pp. 96-97, 26 September 1985.
31. Youngblood, F.L., Characterizing and Controlling the Metallurgical Properties of a Cu-Mn Alloy for Ship Silencing Applications, Master's Thesis, Naval Postgraduate School, Monterey, California, June 1975.

INITIAL DISTRIBUTION LIST

	No. Copies
1. Defense Technical Information Center Cameron Station Alexandria, Virginia 22304-6145	2
2. Library, Code 1424 Naval Postgraduate School Monterey, California 93943-5000	2
3. Professor Jeff Perkins, Code 69Ps Department of Mechanical Engineering Naval Postgraduate School Monterey, California 93943-5000	3
4. LCDR Kenneth P. Roey 949 Nugent Drive Chesapeake, Virginia 23320	3
5. Mrs. Catherine Wong, Code 2812 David Taylor Naval Ship R&D Center Annapolis, Maryland 21402	3
6. Department Chairman, Code 69Hy Department of Mechanical Engineering Naval Postgraduate School Monterey, California 93943-5000	1
7. Superintendent Naval Postgraduate School Code 34 Monterey, California 93943-5100	1
8. Dr. Ming Wu Memory Metals, Inc. 83 Keeler Avenue Norwalk, Connecticut 06854	1
9. Naval Sea Systems Command Code 92R Washington, D.C. 20362-5101	1